Development of a Procedure to Measure the Effectiveness of Electret N-95 Respirator Filter Media for Capturing Nano-Particles

Reza Mostofi Darbani

A Thesis

in

The Department

of

Building, Civil and Environmental Engineering

Presented in Partial Fulfillment of the Requirements

for the Degree of Master of Applied Science (Civil Engineering) at

Concordia University

Montreal, Quebec, Canada

December 2010

CONCORDIA UNIVERSITY
School of Graduate Studies

This is to certify that the thesis prepared

By: Reza Mostofi Darbani

Entitled: Development of a Procedure to Measure the Effectiveness of Electret N-95 Respirator Filter Media for Capturing Nano-Particles

and submitted in partial fulfillment of the requirements for the degree of

Master of Applied Science (Civil Engineering)

complies with the regulations of the University and meets the accepted standards with respect to originality and quality.

Signed by the final examining committee:

Dr. S. Li Chair

Dr. M. Nokken Examiner

Dr. R. Sedaghati Examiner

Dr. F. Haghighat Supervisor

Approved by Dr. K. Ha-Huy

Chair of Department or Graduate Program Director

Dr. R. Drew

Dean of Faculty

Date Jan 13, 2011

ABSTRACT

Development of a Procedure to Measure the Effectiveness of Electret N-95 Respirator Filter Media for Capturing Nano-Particles

Reza Mostofi Darbani

The phenomenal growth of the nano-technological products and their impacts on our society led government organizations and scientists to consider the risks related to human exposure to nano-particles (NPs). As a precautionary approach, respiratory protection is suggested for workers to reduce their exposure to NPs. Thus, it is important to characterize the performance of these respirators to capture NPs.

In this study, the performance of one model of N95 respirators was characterized against poly and mono-disperse NPs. With poly-disperse NPs, a methodology was developed to measure the performance of the N95 respirators against NaCl aerosols in the size range of 15 to 200 nm in three scenarios. The N95 respirator performance was also characterized at 85 liters/min against twelve mono-size aerosols with size ranging from 20 to 200 nm.

Using poly-disperse aerosols test (PAT) method; the results demonstrated that the initial penetration was significantly enhanced with the increased airflows and a shift toward small particle size was observed for the most penetrating particle size (MPPS). For particles below 100 nm, the penetration decreased with further loading. The MPPS was also found to shift toward the large sized particles. In addition, the penetration augmented slightly as the (RH) increased.

Using mono-disperse aerosol test (MAT) method; the results revealed the initial particle penetration is less than 5% NIOSH certification criterion. However, it was found that the initial value, measured with (MAT) method, is not related with the initial penetration measured with (PAT) method at each corresponding particle size at 85 liters/min.

ACKNOWLEDMENTS

First of all, I wish to express my deepest acknowledgments to my supervisors Dr. Fariborz Haghighat and Dr. Ali Bahloul for all support, research guidance, inspiration and patience over the last two years of my study. Great appreciation is also due to Dr. Jaime Lara; without his continuous support and help, I could not accomplish this research project during my experiments at the IRSST.

I would like to thank other members of this research project; Dr. Bei Wang, Yves Cloutier Roberge Brigitte and Dr. Claude Ostiguy. Much appreciation also goes to technicians Bernard Caron and Pierre Drouinas; for all their technical help to build and develop the set-up.

Many thanks to the Institut de Recherche Robert-Sauvé en Santé et en Sécurité du Travail and Nano-Quebec for supporting this project.

I am also very grateful to all my colleagues at the Concordia University sharing their knowledge and experience while providing me such a friendly environment, so remarkable and worthy.

Finally, I wish to express my deepest appreciation to my dear wife, Mahtab, for her unconditional love, support and perseverance. Special thanks are due to my family, as well, for being always the source of strength, devotion and encouragement.

TABLE OF CONTENTS

LIST OF FIGURES

LIST OF TABLES

LIST OF ABBREVIATIONS

Abbreviation	**Description**
ASHRAE	American Society of Heating, Refrigerating, and Air-Conditioning Engineers
CFR	Code of Federal Regulations
CMD	Count Median Diameter
CV	Coefficient of Variation
DEHS	Di Ethyl Hexyl Sebacate
DHHS	Department of Health and Human Services
DMA	Differential Mobility Analyzer
DOP	Dioctyl Phthalate
DOS	Dicotyl Sebacate
GSD	Geometric Standard Deviation
HVAC	Heating, Ventilating and Air-Conditioning
HEPA	High-Efficiency Particulate Air
K	Kelvin
MAT	Mono-Disperse Aerosol Test
LPM	Liters Per Minute
MPPS	Most Penetrating Particle Size
NaCl	Sodium Chloride
NAFA	National Air Filtration Association

NIOSH	National Institute for Occupational Safety and Health
NP	Nano-Particle
PAT	Poly-Disperse Aerosol Test
RH	Relative Humidity
SCENIHR	Scientific Committee on Emerging and Newly Identified Health Risks
SMPS	Scanning Mobility Particle Sizer
UCPC	Ultra Fine Condensation Particle Counter
UFP	Ultra Fine Particle
V	DMA Voltage
Kr	Krypton

LIST OF SYMBOLS

English Symbols	**Description**
C_{down}	Downstream Concentration
C_{up}	Upstream Concentration
Dp	Particle Size Diameter
K_B	Boltzmann Constant
M	Molecular Weight
P	Particle Penetration
Q	Airflow Rate
q_f	Quality Factor
R	Correlation Ratio
T	Absolute Temperature
Z	Electrical Mobility

Greek Symbols	**Description**
α	Packing Density
η	Total Collection Efficiency
Δp	Pressure Drop

Chapter 1: INTRODUCTION

1.1. Background

The term nano-particles (NPs) basically refers to that range of particles below 100 nm in size, in at least in one axis. NPs can be introduced into the environment from different sources; these can be associated with either natural phenomenon, human or domestic activities (see figure 1-1). There is also a new source of nano-particle emission to the environment known as the engineered NPs which comprises laser ablation, milling, grinding and polishing (Rengasamy, 2008a). However, it is not yet clear to what level these new sources of engineered NPs contribute to the total emissions.

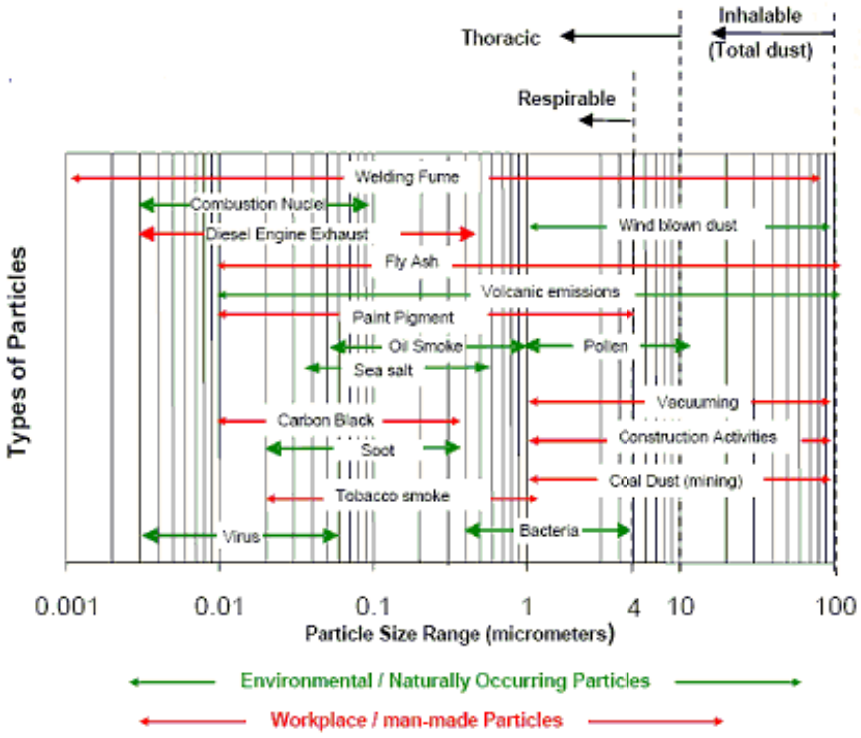

Figure 1-1: Particle source versus particle size. Adapted from Crooks, 2007.

In spite of very low mass concentration, the number of NPs in the environment can be very high. Thus, the human exposure to NPs could be significantly more dangerous to human health than the larger particles. Scientific Committee on Emerging and Newly Identified Health Risks (SCENIHR) (2006) indicated that there could be roughly 10,000 to 20,000 NPs in the air of a normal room and 50,000 and 100,000 NPs per cubic cm in the wood and urban street, respectively. Oberdorster (2005) has also reported the relationship between the particle number concentration, the surface area of particles and the particle's diameter with the same airborne mass concentration of 10 $\mu g/cm^3$ (see table 1-1). As noticed in table 1-1, with the same mass concentration, as the particle size diameter reduces, number of particles would greatly increase along with the exponential growth in particle surface area.

Table 1-1: Number concentration and surface area of particle versus particle diameter. Adapted from Oberdorster, 2005.

Airborne mass concentration	Particle size	Particle number concentration	Particle surface area
($\mu g/cm^3$)	(nm)	(particles/cm^3)	($\mu m^2/cm^3$)
10	5	153,000,000	12,000
10	20	2,400,000	3,016
10	250	1,200	240
10	5,000	0,15	12

Over the past decade, remarkable research has been done to improve the quality and functionalities of products by modifying the characteristics of their material structure at the nano-level. This technology, termed nano-technology, has been applied to the manufacturing of a wide variety of products.

It is believed that workers could be more exposed to NPs during the manufacturing of different products and this could have potential impact to worker's health. According to the Bureau of Labor Statistics and National Institute for Occupational Safety and Health (NIOSH), in 2000 in the U. S., approximately 2 million people worked with nano-material products (NIOSH, 2003). Epidemiological assessments on the ultrafine particles (UFPs), of the same size range as micro-particles, have clearly shown acute and chronic effects related to the exposure to UFPs. Acute toxicity studies on the effects of NPs on animals have also shown acute effects on different organs; however, chronic studies are still very limited and more investigation is vital (Ostiguy et al., 2008).

Findings from the previously mentioned limited toxicological studies demonstrated that for the same mass, under similar conditions, a specific chemical is normally more toxic at the nanometric size range than that at the micrometric size range (Oberdorster, 2000; Donaldson et al., 2001). The toxicity of the NPs was found to escalate remarkably with the increase of the particles' surface area and number concentration (McCullough et al., 1997; Tran et al., 2000). This high surface area results in the higher surface reactivity of NPs which influences their potential toxicity in the presence of more molecules on the surface (Tran et al., 2000; Warheit et al., 2007a; Warheit at al., 2007b).

In general, workers are exposed to NPs through a wide variety of routes in the work environments. These include inhalation, skin absorption, eye contact and ingestion. Inhalation is considered as the most common route which NPs reach the various parts of the living organism. Thus, in order to provide a satisfactory level of safety and health, respiratory protection is suggested for workers against the NPs. When compared with larger particles, a greater portion of inhaled NPs can penetrate into the lung where they are deposited and then translocated to other parts of the body and deposit, such as the brain, blood system, heart, and other organs (Nemmar et al., 2001; Oberdorster et al., 2002; Claude Ostiguy et al., 2008). A portion of these inhaled NPs are translocated to the brain via olfactory and trigeminus nerve, as observed on rats and mice (Oberdorster et al., 2004; Oberdorster et al., 2005). Moreover, they can be transported to the blood system by passing through the pulmonary protection barriers (Takenaka et al., 2001; Nemmar et al., 2002; Oberdorster et al., 2002). In this regard, the toxicity studies in rats and mice have shown that the exposure to NPs causes pulmonary disease, cardiovascular problems and immune system impairments (Dockery et al., 1994; Hagdnagy et al., 1998; Huang et al., 2007).

Wide ranges of engineering control systems have been proposed to reduce or eliminate the exposure to NPs. These systems include enclosures, local exhaust systems, fume hoods, and general ventilation systems.

If engineering controls are insufficient to ensure workers' safety and health, respiratory protection and personal protective equipment using filtration could be used to remove the NPs. The question now is "how effective are these filters to protect workers against

NPs?" The effectiveness of respiratory filters is generally characterized by an airflow rate of 85 liters/min or less. However, few studies have been done on the effectiveness of respiratory protections against NPs at high airflow rates (in the case of respiratory peaks with airflow rates ranging from 300 to 400 liters/min at heavy workloads). The result of earlier (limited) work showed that high airflow rates lead to increase the particle penetration through respirators (Richardson 2006). The effect of other parameters, such as the particle size, humidity and the time of use on the performance of the filter respirators remains also unknown. Therefore, with the exponential growth in the manufacturing sector of nano-products, it is essential to develop a method for measuring the effectiveness of respiratory protections and comparing their performances. To our knowledge, there exists no current standard to quantify or classify the performance of these filters against NPs.

1.2. Research Objective

The objectives of this study are:

- To develop a methodology to characterize the effectiveness of one model of NIOSH-approved N95 respirator against poly-disperse aerosols in size range from 15 to 200 nm in different scenarios:

    1. Investigating the effect of airflow condition and particle size on the initial particle penetration through the respirator and

    2. Investigating the effect of two other parameters, such the time of use and the relative humidity on filtration performance.

- To develop and adapt the experimental set-up to challenge the same type of respirator against mono-disperse particles with a size range between 20 to 200 nm.

1.3. Thesis Outline

Chapter 2 explains the fundamentals of nano-particle filtration and provides critical reviews on the filtration performance of respirators and mechanical filters against NPs. The testing protocol for respirator certification is also presented. Chapter 3 describes and compares two different experimental set-ups for challenging filtering face-piece respirators with NPs. The required procedures to test respirators against mono-disperse and poly-disperse aerosols are discussed in the chapter. Thereafter, the results of calibration and pre-qualification tests will be presented. Chapter 4 illustrates and discusses the experimental results implemented to assess the filtration performance of respirators in different scenarios. Finally, chapter 5 outlines the conclusions and recommendations for future direction.

Chapter 2: LITERATURE REVIEW

2.1. Introduction

Aerosol filtration is one of the most common methods applied for air cleaning and sampling. This method, using fiber filters, is now applied in a wide variety of applications, such as respiratory protection, air cleaning of smelter effluents, processing of nuclear and hazardous materials and clean rooms (Hinds, 1999).

The fiber filters are very efficient and low pressure drop devices for the collection of particles within the small size, due to their loosely packed fibers with the good orientation across the gas flow direction. There are various key factors which affect the efficiency of the fiber filters in capturing particles such as particle characteristics (its physical state, chemical composition, diameter, density and charge distribution), filter characteristics (substrate, fiber diameter, thickness of the filter, packing density of fiber and electrical property), collection mechanisms, operational conditions (temperature, viscosity and filtration face velocity) (Davies, 1973; Dullien, 1989) and thermal rebound due to Brownian motion.

Particle removal is mainly performed by two major mechanisms; mechanical and electrostatic mechanisms. The mechanical mechanism is associated with inertia, gravitational, interception and diffusion caused due to the effect of Brownian motion. However, compared with the other mechanical mechanisms, the inertia and gravitational mechanisms are normally ignored and not significantly considered in calculations for

capturing small particles; these two mechanisms are more dominant to capture the large size particles (basically above 0.5μm). Meanwhile, the effect of Brownian motion becomes more important for particle collection within very small nano size range, particularly below 10 nm (Brown, 1993; Hinds, 1999). On the other side, the electrostatic attraction force is the other collection mechanism; mainly due to Coulombic, image and dielectrophoretic forces between the fiber filters and particles (Davies, 1973). The parameters which can affect the filtration performance with the help of the electrostatic attraction are the amount of charge on the particles, surface charge density of fibers and the electric field applied externally (Wang, 2001).

Recent investigations show that, with the aid of both mechanical and electrostatic mechanisms, the filtration efficiency would significantly improve in particle collection (Balazy et al. 2006a; Huang et al., 2007; Eninger et al., 2008). The electret filters (use the electrostatic forces for particle removal) were firstly developed by Nicolaig Louis Hansen for particle removal (Davies, 1973). Hansen found the electret filters are more effective than the mechanical filters in capturing particles. Rather than increase the filtration performance, the electret filter media offers lower airflow resistance than the mechanical filters, due to its low packing density.

2.1.1. Particle Filtration Mechanisms

Previous research suggested that filtration efficiency can be affected by several parameters such as particle characteristics (e.g., its chemical composition, diameter and density), filtration face velocity (based on airflow rate and filter‘s surface area), the filter characteristics (e.g., fiber diameter, thickness, fiber packing density and porosity),

filtration mechanisms and operational conditions (temperature, relative humidity and viscosity) (Davies, 1973; Dullien, 1989).

As discussed earlier, particle removal is performed by four main collection mechanisms: (1) inertia impaction, (2) interception, (3) diffusion and (4) electrostatic attraction, as illustrated in figure 2-1 (Hinds, 1999). The first three collection mechanisms refer generally to mechanical filters and are influenced by particle size.

- "Inertia impaction occurs when the particle near a filter fiber changes in streamline direction and collides with the fiber" (DHHS, 2003). This collection mechanism becomes more important for capturing the large particles and increases at the higher face velocities.

- "Interception occurs when a particle follows a certain gas streamline and comes within one particle radius of a filter fiber" (DHHS, 2003). Soon after, the particle touches the fiber; it will be removed from the gas flow.

- "Diffusion occurs when the random motion of the particle due to Brownian motion causes the particle to touch the fiber filter" (DHHS, 2003). The diffusion is dependent on the face velocity and the particle size as well. At lower face velocities, the diffusion becomes more dominant, because the particle has more time for zigzag motion, thus the more chance to collide and being captured by the fiber filters. Moreover, the small size particles have more chance to be captured by this mechanism, since they behave like the gas molecules causing more random motion.

- The electrostatic mechanism which plays a significant role in electret filters is due to electrostatic attraction between the particles and the fiber filters; mainly as a result of the Coulombic, image and dielectrophoretic attraction forces.

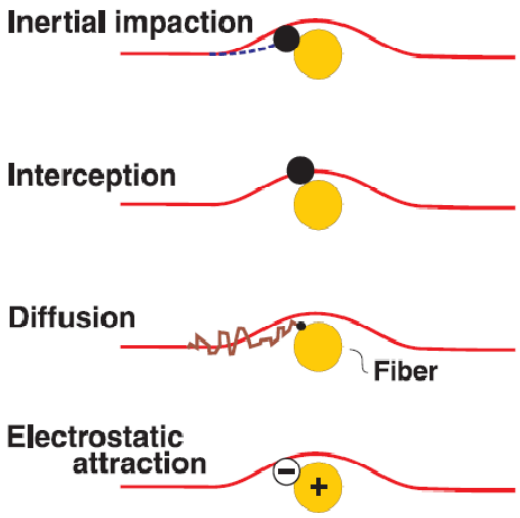

Figure 2-1: Four primary particle collection mechanisms of particle capture. Adapted from DHHS, 2003.

However, for nano-sized particles, the inertia mechanism does not significantly contribute to the capturing mechanisms and are thus not considered in calculations as they are more predominant on the collection of the larger size particles. Also note that the effect of Brownian motion is more significant as the particles become smaller, particularly for the particles within the nano size ranges (Brown, 1993; Hinds, 1999).

Figure 2-2 illustrates the combined effect of the first three mechanisms (inertia impaction, interception and diffusion) on the particle collection as a function of the particle diameter. In general, diffusion is considered as the predominant collection

mechanism for particles less than 200 nm, while the interception and inertia impaction are dominant for the particles larger than 200 nm.

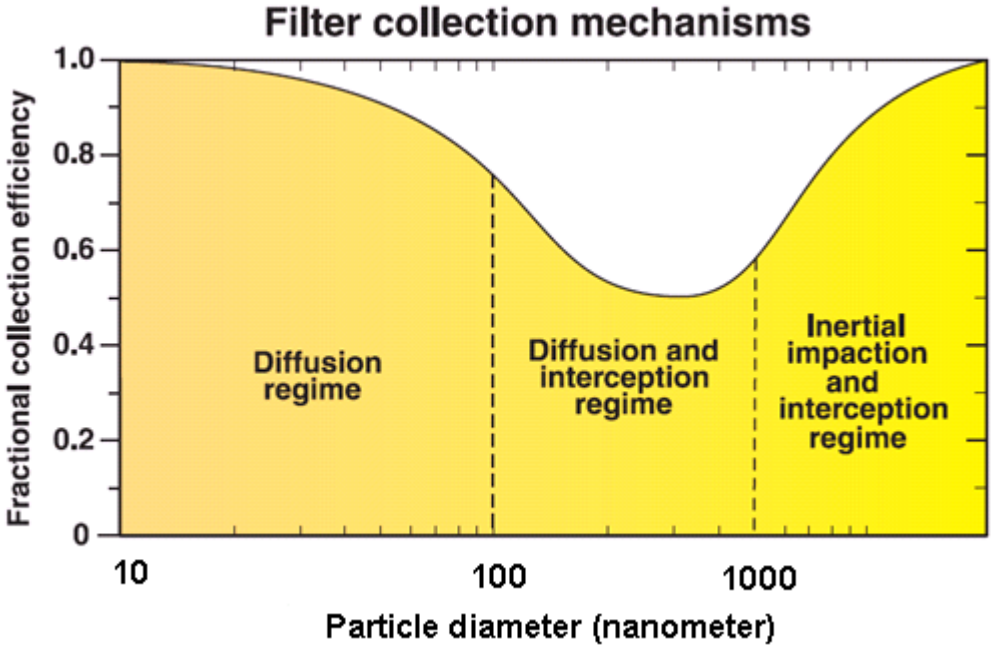

Figure 2-2: Fractional collection efficiency versus particle diameter for a mechanical filter. Adapted from Lee et al., 1980.

Figure 2-2 also demonstrates that for particles below 100 nm filtration efficiency will enhance as the particles become smaller. This is due mainly to the fact that diffusion mechanism is dominated in this region. For particles with diameter between 100 to 400 nm, both diffusion and interception contribute to the removal of particles by filters. However, in this region, the filtration efficiency is markedly reduced, as the particles are not small enough to be captured by the diffusion effect and not too large to be captured by impaction mechanism. This region is generally considered the worst-case situation; this size range experiences the greatest penetration through the filter. And finally, for

particles larger than 400 nm, the filter performance will increase again as both the interception and inertia impaction effects significantly contribute to the collection of particles (Lee et al., 1980).

However, it should be mentioned that in the classic collection efficiency curve, for the elecret respirator filters, the minimum filtration efficiency, for the most penetrating particle size (MPPS), can be shifted toward small particle sizes lower than 100 nm (Han, 2000; Martin and Moyer, 2000; Huang et al., 2007; Rengasamy et al., 2007; Eninger et al., 2008).

2.2. Personal Protective Equipment

The fibrous filters produce low-pressure drop and remove particles randomly laid perpendicular to the airflow (see figure 2-3). Fibers are commonly made of cotton, ceramic, fiberglass, polyester, polypropylene, polycarbonate or numerous other materials which can be synthesized in both charged and uncharged filters (Davies, 1973).

Basically, in terms of filtration mechanism, two types of fibrous filter media including: (1) mechanical filters and (2) electrostatic filters (electret filters) can be used in aerosol filtration. In mechanical filters, inertia impaction, interception and diffusion mechanisms contribute to the particle collection, while, in electret filters, the electrostatic attraction is additionally applied to enhance the collection efficiency. In addition to higher collection

efficiency, in electret filters, with the aid of this extra mechanism, a lower pressure drop across the filter occurs due to low packing density[1].

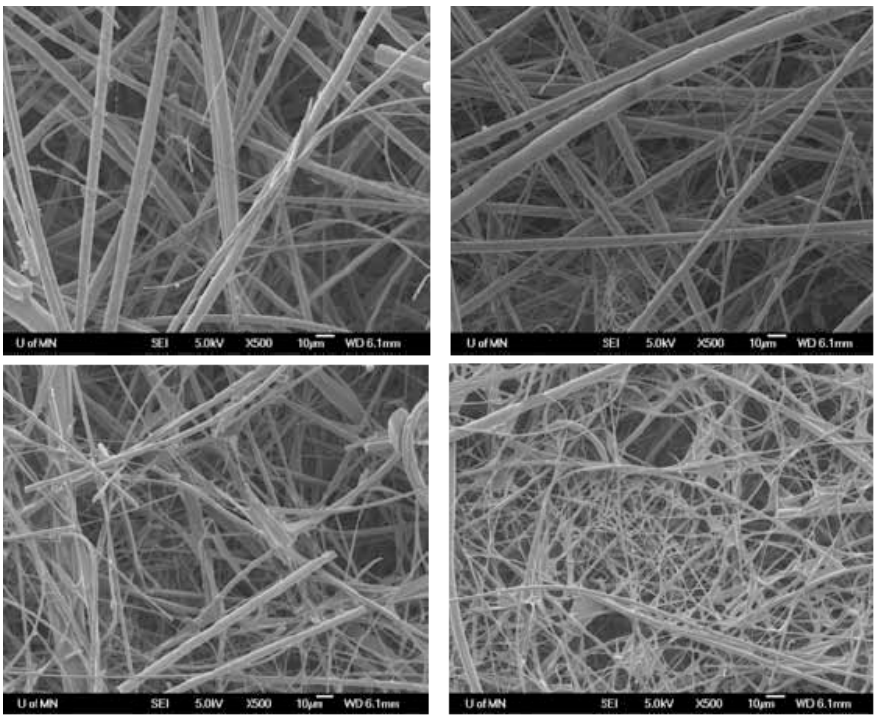

Figure 2-3: The image of various fibrous filter media by scanning electron microscope. Adapted from Pui et al., 2006).

Earlier studies also have indicated that the filtration mechanisms, mechanical and electrostatic, can influence the performance of the fibrous filters in particle collection within the nano-sized range. In mechanical filters both filtration efficiency and the air resistance curve basically increase with respect to operating time. While in electret filters

[1] The packing density is defined as the percentile ratio of fiber volume in the filter to total filter volume, typically ranges from 1 to 30% (Davies, 1973).

this tendency moves in the inverse directions. During the filter loading, the electrostatic effect between the particles and the filter is gradually diminished since more particles are penetrated through the filter leading to less filtration performance. However, at a certain point, the filtration performance cease to reduce and rise again, as the mechanical mechanisms contribute much more to capture the particles: at this point, the deposited particles on the filter medium surface behave as a very efficient layer to collect particles by the mechanical mechanism forces.

Moreover, according to the literature, in contrast with mechanical filters, for electret filters, the lowest filtration efficiency occurs at smaller particle sizes normally between 40-60 nm (Han, 2000; Martin and Moyer, 2000; Huang et al., 2007; Rengasamy et al., 2007; Eninger et al., 2008). However, for mechanical (non-charged) filters, a particle diameter of 300 nm is referenced as the Most Penetrating Particle Size (MPPS) at 85 liters/min. In this regard, the particle penetration through both mechanical and electret filters were investigated for the particle size range from 4.5 nm to 10 μm by Huang et al. (2007). They reported that the maximum penetration was reduced from 18.9 to 5.8% with the co-operation of an electrostatic attraction force in particle collection. In addition, their study demonstrated that the MPPS shifts toward the smaller size by using electret (pre-treated) filters. The MPPS occurred at 50 nm for electret and 200 nm for mechanical filters.

Balazy et al. (2006a) also measured the penetration of the MS2 viruses (a non harmful stimulant of several pathogens) through filtering face-piece respirators. Their study was carried out for particles ranging from 10 to 80 nm and at the airflow rates of 30 and 85

liters/min. They reported that the penetration through the electret N95 respirators can exceed up to 5.6% in the MPPS at 85 liters/min, simulating an average inhalation rate for heavy workload conditions. However, N95 respirators are expected to provide 95% minimum filtration efficiency against non-biologic and biologic particles in the MPPS. It was also acknowledged that the MPPS lies within the smaller particle size of approximately 50 nm. While, the earlier results show that the MPPS diameter can be highly variable due to the filter's property, filtration mechanism, airflow rate, etc.

2.3. Factors Affecting Particle Filtration

2.3.1. Face Velocity and Airflow Rate

The face velocity / airflow rate can significantly affect the total filtration performance of fibrous filters since they influence the contribution of diffusion, interception and electrostatic mechanisms to the particle collection (Kousaka et al., 1990; Alonso et al., 1997). At low face velocities, diffusion and electrostatic forces contribute significantly to the capture efficiency due to a higher residence time. With an increasing face velocity, the interception mechanism dominates while the diffusion effect contributes much less to the filter's collection performance. Thus, it is expected that the filtration efficiency for small particles drops markedly at higher face velocities.

For the mechanical filters, particle penetration is presented as a function of the face velocity. Steffens and Coury (2007) studied the effect of velocities varying from 3 to 25 cm/sec on the filtration efficiency, using homogeneous and heterogeneous fiber filters, for the particle size between 8.5 to 94.8 nm in diameter. Their experimental results

implied that the filtration performance would reduce with increasing the filtration face velocity. Boskovica et al. (2008) tested the filtration efficiency at various velocities ranging from 5 to 20 cm/sec for different shapes of particles (sphere, semi rounded and cubic). The results in all cases showed that at lower face velocities the filtration efficiency of fibrous filters improved for all different shape of particles. Balazy et al. (2004) investigated the filtration efficiency and pressure drop for face velocities between 10 and 30 cm/sec. Their experimental data demonstrated that increase in air filtration velocity would lead to lower collection efficiency. This finding supports the dominance of diffusion mechanism of particle removal in the nano-sized range. Kim et al. (2007) also conducted the penetration test at three face velocities of 5.3, 10 and 15 cm/sec using silver NPs from 3 to 20 nm. The results showed that a higher face velocity would increase particle penetration due to the shorter residence time through the filters.

For respirator filters, particle penetration is determined as a function of the airflow rate instead of that of the face velocity. Several studies have been conducted to investigate the effectiveness of respirators in the removal of NPs under different airflow rates. Eninger et al. (2008) evaluated the performance of one N95 and two models of N99 face-piece respirators against three viruses and NaCl particles in the size range of 20 to 500 nm. The test was carried out at airflow rates of 30, 85 and 150 liters/min. The highest NaCl particle penetrations of 1.3, 5.9 and 10.2% for N99A respirator and 1, 4.3 and 6.6% for N99B respirator were observed at airflow rates of 30, 85 and 150 liters/min, respectively.

For the N95 model, the highest NaCl penetrations were 1.4, 4.8 and 8.1% for airflow rate of 30, 85 and 150 liters/min, respectively. For the viruses, an increase in the airflow rate

from 85 to 150 liters/min strongly affected the performance of all tested respirators (N99A, N99B and N95). Balazy et al. (2006b) also measured the penetration through two models of N95 respirators for NaCl particles within the 10 to 600 nm range at two airflow rates of 30 and 85 liters/min. The airflow rate demonstrated a strong impact on particle penetration through filtering face-piece respirators. Particle penetration through the both N95 respirators would be exceeded 5% at airflow rate of 85 liters/min. Furthermore, the performance of several N95 and P100 models against mono-disperse silver aerosols were evaluated by Rengasamy et al. (2008a). The test was carried out for particles ranging from 4 to 30 nm at airflow rate of 85 liters/min. Particle penetration decreased for all tested respirators as the particle size decreased to 4 nm. For N95 filtering face-piece respirators, particle penetration varied from 1.1 to 4.0%. Finally, for P100 respirators, particle penetration less than 0.003 was observed with MPPS between 40 to 50 nm.

The majority of previous investigations suggested testing filtering face-piece respirators at the rate of 85 liters/min, however, it has been recommended that respirators should be tested at an airflow rate of 350 liters/min simulate human breathing at a heavy work load; it is believed much higher breathing airflow rate may occur in the workplace (Janssen et al. 2003; Balazy 2006b).

2.3.2. Thermal Rebound Effect

From the prediction of the theoretical models, particle collection efficiency should increase as the size of the particle is reduced. However, some recent studies indicate that the collection efficiency of nano-sized particles can be significantly reduced due to the possibility of thermal rebound effect. It has been stated that with the reduction of the

particle size below a certain point, the mean thermal velocity due to Brownian motion exceeds the capture velocity on particles, and consequently increases the likelihood of particle detachment from the filter surface (Brown, 1993). On the other hand, particles of decreasing sizes would have lower adhesion ability when they come in contact with filter surfaces due to their behaviors: they behave more like molecules. Brown observed that as nano-sized particles approach the dimension of molecular clusters and when they undergo contact with a fiber surface they would not adhere to it (Hinds, 1999). However, there is very limited information on the exact particle size from which such rebound effect begins to occur.

Several researchers have examined the effect of thermal rebound on the particle penetration through filters. Wang and Kasper (1991) confirmed the occurrence of the thermal rebound phenomena in aerosol filtration of the particles smaller than 10 nm. They showed that the thermal rebound velocity increases the capture velocity of particles with size varying from 1 to 10 nm, causing the particle collection efficiency to drop for particles smaller than 10 nm. Furthermore, in considering the effect of particle bouncing due to the thermal rebound velocity, they developed a model to predict the filtration efficiency of particle size in the thermal rebound regime. Otani et al. (1994) examined particle penetration through a circular tube for silver particles below 2 nm. The results showed a higher particle penetration through the tube at smaller particles. Similarly, Balazy et al. (2004) investigated the particle penetration through the filters for liquid di-ethyl-hexyl-sebacate (DEHS) particles below 20 nm. They concluded that the collection efficiency of the particles was also dramatically reduced as the particle became smaller than 20 nm. Ichitsubo et al. (1996) found that the collection efficiency of the particles

was lower than that predicted by the theoretical model for the particles with sizes below 2 nm: this could be likewise due to thermal rebound effect. Kim et al. (2006) studied the filtration efficiency of two different types of glass fibrous filters on collection of NaCl particles at room temperature. They pointed out that the thermal rebound effect occurred at particles sizes below 2 nm and the electrostatic effect significantly enhanced in this regime. However, Alonso et al. (1997) detected no particle rebound phenomenon in the same size range as that investigated by Ichitsubo et al. (1996). They reported that the disagreement between the theoretical and experimental studies was attributed to an unreliable sizing of the particles below 3 nm with the currently available techniques.

Huang et al. (2007), measuring the penetration in the size range between 4.5 nm to 10 μm NaCl aerosol particles through face-piece respirators, observed no thermal rebound phenomena. Japuntich et al. (2007) measured the filtration efficiency of particles in the size range of 10 to 400 nm and found no thermal rebound. Rengasamy et al. (2008a) investigated the filtration performance of five models of NIOSH-approved N95 and two models of P100 face-piece respirators against mono-disperse silver and NaCl NPs. They reported that the penetration levels of silver particles decreased with particle diameter down to 4 nm for all five N95 models and down to 12 nm for two P100 models, which was consistent with the single-fiber filtration theory. They claimed that there was no evidence for thermal rebound effect for particles in the size range of 4 to 30 nm.

Shin et al. (2008) detected no thermal rebound in the investigation of the filtration efficiency of silver nano-particles between 3 to 20 nm at temperatures up to 500 K. According to the study conducted by Wang and Kasper (1991), more particle detachment

from the fiber surface was expected as a result of exceeding the Brownian motion of NPs at elevated temperatures compared to room temperatures would be observed. They reported the possibility of thermal rebound at high temperatures for NaCl particles within the 1 to 3 nm size range. However, no particle bouncing was reported even at elevated temperatures. Shin et al. (2008) asserted that the inconsistency from two studies might be attributed to the different behavior of silver particles at elevated temperature when compared with behavior of NaCl particles. Wang and Kasper (1991) reported the possibility of thermal rebound at high temperatures for NaCl particles with a 1 to 3 nm diameter range.

2.3.3. Relative Humidity

Relative Humidity (RH) is one of the factors that may influence filtration performance. The effect of humidity is not yet well understood due to a lack of investigations. Kim et al. (2006) reported no significant effect of humidity on filtration efficiency for particles smaller than 100 nm; showing almost the same filtration efficiency at different tested (RH) of 0.04, 1.22 and 92%. Contrary to Kim et al.'s observation, Brown, (1993) and Miguel, (2003) reported higher filtration efficiency for the fiber filters with an increase in (RH) but for coarse particles. This phenomenon is attributed to particle adherence to the fiber filter and collected particles due to increase in capillary force at higher (RH). However, the attraction between particles and fiber filters due to capillary force is only considerable for large size particles.

In contrast to earlier studies on mechanical filters, the studies for the electret filters (charged filters) showed lower performance with increase of the (RH), due to the

reduction in the charges on the fiber filters and particles with an increase in (RH) (Ackley, 1982; Moyer et al., 1989). Ikezaki et al., (1995) and Lowkis et al. (2001) also confirmed that the potential of the electret filters to collect the particles decrease as the surface charge was decreased with increase of the (RH). Yang and Lee (2005), however, reported that (RH) had no effect on aerosol penetration through the electret (pre-treated) filters. They implemented the filtration test at different (RH) of 30 and 70% for mono-disperse generated NaCl particles size ranging from 50 to 100 nm.

2.3.4. Particle Loading

Particle loading is one of the other important aspects which influence the filtration performance. The feedback effect of particle loading is less well understood. According to the literature, the subsequent particle loading implies a significant impact on the collection efficiency and also pressure drop evolution across a filter (Baumgartner et al., 1986; Brown et al., 1988; Chen et al., 1993; Martin and Moyer, 2000; Wang et al., 2001). With the absence of the electrostatic effect, the continuous particle loading generally results in an increase in the particle collection efficiency and pressure drop, caused by the particle accumulation on the fiber surface (Wang, 2001).

In contrast with results obtained for the mechanical filters, according to the previous experimental studies on the electret filters, the particle penetration level mostly propagates during the initial stage of filter loading (Baumgartner et al., 1986; Brown et al., 1988; Chen et al., 1993; Martin and Moyer, 2000; Wang et al., 2001). However, the pattern for particle collection efficiency may change by different fiber materials and particle size. Chen et al. (1993) investigated the filtration performance of dust-mist

filtering face-pieces loaded continuously against corn oil aerosols with size diameter of 0.16 μm. They reported that the particle penetration initially increased with aerosol loading due to reduction in electrostatic charge effect, whereas subsequently diminished due to the increase in packing density of the fiber filter. Brown et al. (1988) reported that the filter loading would significantly augment the penetration through the electret filters, since the electrostatic charge effect on the filter fiber is screened by the deposited aerosols. Their experiments were carried out for various industrial aerosols at different particle size ranges.

Additionally, experimental studies on electret filters showed that the particle collection efficiency relies generally on the manner in which the particles are collected; exposed with solid or liquid particles (Martin and Moyer, 2000; Ji et al., 2003). Martin and Moyer (2000) used solid NaCl and liquid DOP particles to test the filtration efficiency of N95 respirators. Their results indicated more particle penetration when the N95 respirator was challenged with the liquid DOP aerosols; increased by about ten folds. In another study conducted by Ji et al. (2003), the electret filters were loaded with poly-disperse solid sodium chloride (NaCl) and liquid dicotyl sebacate (DOS) particles. In consistent with the other study, much lower filtration performance occurred with testing filters against liquid dicotyl sebacate (DOS).

2.3.5. Particle Charge State

Particle charge is another factor that significantly affects the particle filtration efficiency of mechanical and electret filters (Fjeld and Owen, 1988; Chen et el. 1998). The increase in filtration efficiency is associated with additional electrostatic attraction resulting from

coulombic and image force attraction (Brown, 1993). Kim et al. (2006) demonstrated the difference in the collection efficiency through a glass fiber filter at different charge states for particle ranging from 2 to 100 nm. They found that the filtration efficiency for uncharged particles was much lower than that for charged particles, and this discrepancy decreased with the reduction in particle size. They explained that this phenomenon was due to the fact that diffusion is the most dominant deposition mechanism for nano-particles and this process increases the effect of diffusion for smaller particles. Penetration of neutralized and non-neutralized particle in the range of 10 to 600 nm through electret and mechanical filters was also investigated by Balazy et al. (2006b). In their study, higher filtration efficiency was observed when testing the penetration of neutralized particles for electret filters. However, for the mechanical filters, they reported no significant change between the neutralized and non-neutralized particles. Yang and Lee, (2005) also measured the particle penetration with Boltzmann-equilibrium, neutral (uncharged) and singly charged NaCl aerosols. Their results showed that the singly charged aerosols would lead to higher filtration efficiency than neutralized aerosols: the Coulombic force was dominant in the capture of small particles below 100 nm.

It is very difficult to draw a scientific conclusion from the prior studies investigated the effect of various parameters on the filtration efficiency. These were carried out at various conditions (temperature, airflow rate, RH, measurement techniques, etc.) and indicate that there is a lack of understanding on the effectiveness of filtering face-piece respirators for capturing NPs, and an absence of a standard procedure to measure the respirator filter's effectiveness. Prior studies were limited to relatively low airflow rates. Hence, the results cannot be inferred for real applications. With an increased emergence of nano-

technologies, it is essential to develop a test method to characterize the effectiveness of various respirator filters and to study the impact of above-mentioned parameters on their effectiveness under conditions normally found in work environment. Personal protective equipment filtration devices can play a significant role in reducing or eliminating the exposure to NPs in a work place.

The majority of previous investigations on respiratory protective devices (for example, filtering face-piece respirators) were conducted at constant airflow rates ranging between 30 and 85 liters/min. Although airflow rate of 85 liters/min simulates the relative high breathing rate at strenuous workload used by NIOSH for respirator certification, it is believed that the inhalation flow rate can exceed 350 liters/min at heavy workload (Janssen, 2003; Balazy et al. 2006b).

2.4. Standards for the Filter Performance Evaluation and the Limitations

Recently, from June 1995, the National Institute for Occupational Safety and Health (NIOSH) has certified the Non-Powered Air-Purifying Particulate Respirators in accordance with title Code of Federal Regulations, part 84 (42 CFR 84), replaced with 30 CFR part 11 (CFR, 1996). In this updated regulation, in terms of the type of challenge aerosols, solid and oily aerosols, the filters are categorized in three classes of N, R and P respirators with three levels of filter efficiency, 95, 99 and 99.97% for each class of filters. N type of respirators correspond to the filters with resistance against only solid aerosol (not efficient against oily aerosols), while the R and P type respirators are also intended to be fairly and highly resistant, respectively, against oily aerosols. NIOSH

approves the ‘N-series’ respirator filters with a poly-disperse NaCl particles with a count median diameter (CMD) of 75±20 nm and a geometric standard deviation (GSD) not greater than 1.86. And the R- and P- designated respirators are challenged against dioctyl phthalate (DOP) with CMD of 165±20 nm and a GSD not further than 1.60 (CFR, 1996).

The existing certification NIOSH intends to certify the N, R and P respirators at very conservative test condition, as the performance of the filter can tremendously vary under different situations. For instance, to test filters in a severe condition, the respiratory tests in NIOSH are performed at a constant airflow rate of 85 liters/min corresponding to an average breathing rate of an individual involved in a heavy work load.

However, this certification tests may be used for ranking of respirators but may not always represent the worst case scenario in terms of the collection efficiency (Eninger et al., 2008). For example, Balazy et al. (2006b) showed that an emerging Coulombic force would be induced if both filters and particles were charged: this would significantly overestimate the respirator performance. As pointed out earlier, the MPPS for a specific filter system, can be shifted mainly depends on the magnitude of filtration face velocity, filter‘s type, filtration mechanism, fiber charge density and particle charge distribution (Eninger et al., 2008). The MPPS for electret filters is much smaller than that for mechanical filters. However, the NIOSH certification test assumes the MPPS of approximately 300 nm for all filters and filters types: which may not be true for electret filters. Furthermore, forward-light scattering photometers are used in the NIOSH testing protocol to measure aerosol concentrations before and after the tested respirator. Generally, photometer signal is only capable of measuring the particles with diameters

larger than 100 nm such that photometric method deployed in the NIOSH protocol is not suitable for measuring the filtration efficiency for nano-particles (Eninger et al., 2008). In a study carried out by Eninger et al. (2008), the results showed 68% (by count) and 8% (by mass) of NaCl and 10% (by count) and 0.3% (by mass) of DOP particles are below 100 nm in NIOSH testing protocol. However, as noted above, the photometric method used in NIOSH protocol does not effectively contribute to measure the ultrafine particles (<100 nm). One of the other limitations in NIOSH certification is that the collection efficiency of the filter respirators is not presented in terms of the particle size; the test is only based on measuring particle mass concentration before and after filter for poly-disperse challenge aerosols. However, as discussed previously, in spite of very low mass concentration, the number of NPs can be very high in the environment. Thus, the human exposure to NPs can be even more dangerous to human health than the larger particles.

Chapter 3: EXPERIMENTAL METHOD AND SYSTEM CALIBRATION

3.1. Introduction

This chapter describes a small scale test facility used in this research to develop a "test procedure" to evaluate and compare different devices. The test system was designed and constructed to incorporate an air-cleaning device to simulate its actual application. The duct was made of a stainless steel chamber with a Plexiglas opening in the front and back. Air supplied to the system was filtered through a HEPA filter and conditioned to have constant temperature and humidity. A HEPA filter was used at the end of the unit to remove particles before discharging the air. Thus, the pump must be capable of providing the design airflow rate against the system pressure drop.

In this chapter, according to the air filter test methodology, the schematic diagram of two experimental setups are discussed and compared for challenging filters against NPs, as shown in figures 3-1 and 3-2. These schematic diagrams express the required procedures to test respirators against mono-disperse and poly-disperse aerosols utilized in different scenarios, respectively. Thereafter, the required test procedures and results related to the calibration and qualification tests are illustrated.

3.2. Overview of Experimental Set-up

3.2.1. Filtration Test against Mono-Disperse Aerosols

The six-Jet Collision Nebulizer (Model CN25, BGI Inc., Waltham. MA) is employed as an aerosol generator to provide particles with a size ranging from 15 to 200 nm (see figure 3-1). Next, a long differential mobility analyzer (long DMA) (Model 3081, TSI Inc.) is used to extract mono-sized particles by size classifying the charged particles based on their electrical mobility[2]. As the particles enter the DMA, they experience an external electric field causing each particle with a certain diameter to follow a specific trajectory and to migrate with a certain amount of velocity. Only specific size-selected particles within a narrow range of electrical mobility (inversely related to particle size) will have the correct trajectory to exit the DMA. Then, the resulting charged particles of known size exiting from the DMA are passed through the neutralizer (Kr-85) (Model 3012A, TSI Inc.) to obtain the Boltzmann charge equilibrium. Afterwards, according to the testing airflow rate, an extra dry- filtered airflow is added to the mono size selected aerosol flow. The total aerosol flow from the DMA and the extra introduced clean air are mixed before entering the filter test system. In addition, a small mixing fan is used at the inlet of the chamber to disperse the aerosols. An ultra fine condensation particle counter (UCPC) (Model 3775, TSI Inc.) is then used to monitor the particle concentration in real time at the downstream and upstream of the filter alternately. And consequently, the

[2] The electrical mobility is the ratio of migration velocity caused by an external force, an electric field, to the magnitude of the external force.

filtration efficiency at the tested particle size is measured. By performing the test for different mono size particles, the particle filtration efficiency (or particle penetration) can be determined as a function of particle size.

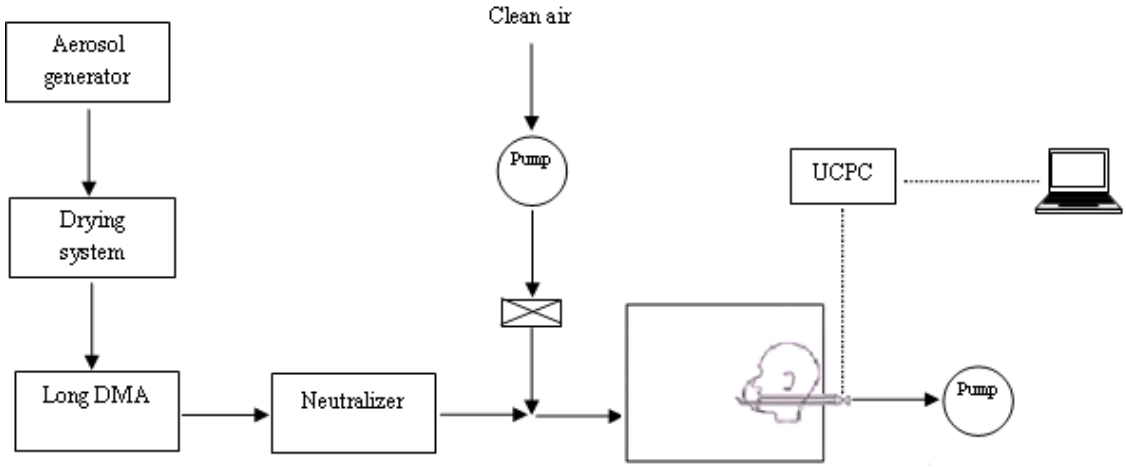

Figure 3-1: Schematic diagram of experimental set-up: testing filters against mono-disperse aerosols. Manikin adapted from Balazy et al., 2006a.

3.2.2. Filtration Test against Poly-Disperse Aerosols

In this experimental set-up (see figure 3-2), after generating poly-disperse aerosols and passing the generated aerosols through the neutralizer, the additional required dry-clean airflow is added to the neutralized poly-disperse aerosols. Next, the mixed poly-disperse aerosol and airflow is passed directly into the chamber. The Scanning Mobility Particle Sizer (SMPS) (Model 3936, TSI Inc), which mainly consists of DMA and CPC, is then used to scan the particle size distribution both at the downstream and upstream of the filter, alternately. Consequently, the particle collection efficiency (or particle penetration) is determined as a function of particle diameter.

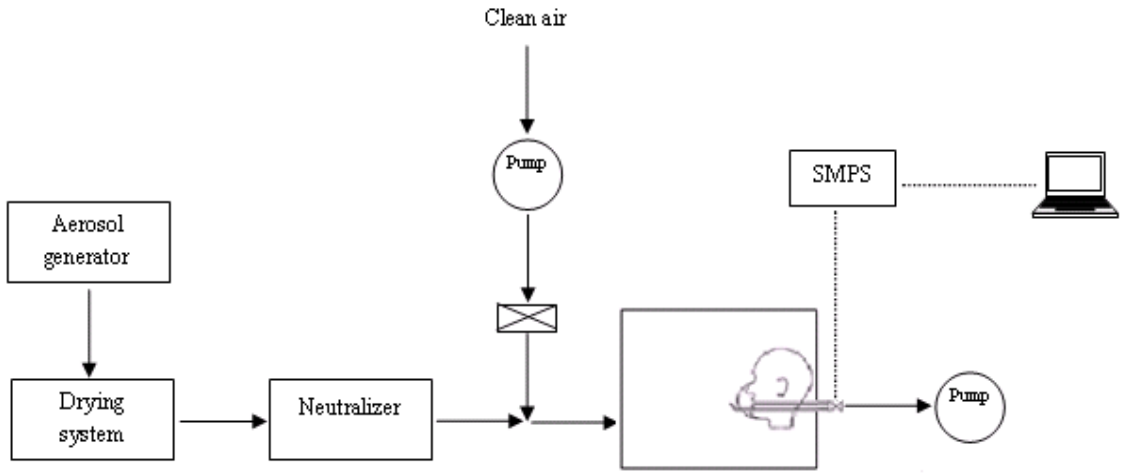

Figure 3-2: Schematic diagram of experimental set-up: testing filters against poly-disperse aerosols. Manikin adapted from Balazy et al., 2006a.

3.3. Test Procedure

Figure 3-3 presents the full schematic of the experimental set-up utilized to challenge tested respirators against poly-disperse aerosols. The test system was first set-up and calibrated according to the requirements of the ASHRAE testing standard 52.2 (2007) (see section 3.5 related to the calibration tests).

Figure 3-3: Schematic of the test system used to challenge N95 respirators against poly-disperse aerosols.

In the case of respiratory filters, one model of NIOSH- approved N95 filtering face-piece respirators was selected to challenge against poly-disperse NPs (see figure 3-4). The selected N95 respirator was sealed by silicon sealant on the manikin's face and placed on the left side of the test chamber (see figure 3-5). Considering this situation, the possible leakage through the respirators and manikin's face was not taken in the filtration efficiency analysis.

Figure 3-4: Photograph of the tested N95 respirator.

Figure 3-5: Photograph of the N95 respirator sealed on the manikin.

The six-Jet Collision Nebulizer was operated at an inlet pressure of 25 psi, and fed with 0.1% (V/V) NaCl solution to generate poly-disperse NaCl particles in the 15 to 200 nm range. The challenge NaCl aerosol employed in this study, with 99.9% purity and density of 2165 kg/m^3, was dissolved in distilled water and alcohol. A filtered air supply (Model 3074, TSI Inc.) was used to provide a clean-dried air entering the generation system (see figure 3-6).

Figure 3-6: Photograph of the filtered air supply (Model 3074, TSI Inc.) connected with six-Jet Collision Nebulizer.

Prior to the filtration efficiency test, in order to reach a steady state concentration at the upstream of the chamber, the generation system was allowed to operate for at least 5 minutes (for more detailed information, review the calibration results for the stabilization test). To reduce the chance of particle loading, the N95 respirator was bypassed during the stabilization period. Having stabilized the system, the switching valve was adjusted, letting the total aerosol flow pass directly through the test filter.

Subsequently, after allowing the system to stabilize and setting the sampling flow rate at 1.5 liters/min, the concentration and size distribution were measured alternately twice at the downstream and twice at the upstream of the test filter by a SMPS. The required time for each measurement at either downstream or upstream was 135 seconds. Consequently,

the particle penetration values were determined as a function of particle diameter. The particle concentration and size distribution at airflow rates of 85, 135, 270 and 360 liters/min at upstream (used for challenging the N95 respirator against poly-disperse aerosols) are presented in figure 3-7.

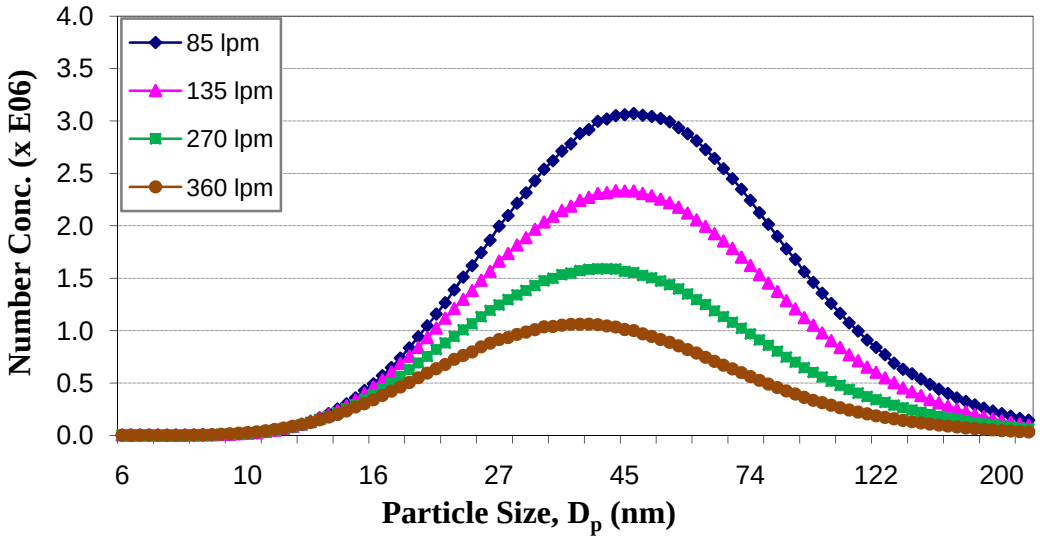

Figure 3-7: The particle concentration and size distribution of the challenge NaCl aerosol at different testing airflow rates (operating Nebulizer at 25 psi inlet pressure, using 0.1% NaCl solution).

In the experimental set-up, a pressure transducer was also applied to measure the pressure drop across the tested face-piece respirator. Thus, the quality factor (q_f)[3], which

[3] The quality factor is used as a means to categorize the filter performance in accordance with particle penetration and air resistance (Hinds, 1999).

corresponds to the particle penetration (P, %) and airflow resistance (Δp, in mm H2O) through the filter, was determined based on the particle size. This indicator of filter performance is defined as:

$$q_f = \frac{\ln(1/P)}{\Delta p} \qquad (3-1)$$

The selected N95 respirator was not preconditioned for relative humidity before testing (filters were tested as received from the manufacturer). According to the 42 CFR 84, pre-treatment at 85% relative humidity and 38° C for 25 hours is required for N series respirators. Additionally, the operational conditions (temperature, pressure and relative humidity) were monitored in the chamber during the test. The temperature was maintained at the ambient temperature (23±2°C) and the relative humidity (8±2%). In addition, a small mixing fan was housed at the inlet of the chamber.

To remove the possible water vapour in the aerosol flow coming out from the Collision Nebulizer, a diffusion dryer was applied. The drying system was composed of an inner tube made of a wire screen and surrounded by silica gel in an outer plastic tube (see figure 3-8). In this case, as the aerosol passed through the inner tube, the water vapour was absorbed on the porous wall and afterwards removed with the surrounding silica gel.

Figure 3-8: The silica gel drying system.

To challenge N95 respirators against mono-disperse aerosols, the same testing procedure as discussed above was followed, except the experimental set-up was adapted to be capable of testing filters with mono-disperse particles (see figure 3-1).

After generating poly-disperse aerosols using the six-Jet Collision Nebulizer (operated at an inlet pressure of 25 psi, using 0.1% NaCl solution) and passing the generated aerosols through the silica gel drying system, a long DMA was utilized to extract mono size particles before entering the filter test system.

A UCPC was used to count the particle concentration of each selected mono-sized particle at both the downstream and upstream of the filter. The challenge mono-sized

NaCl aerosols were pumped for 2 minutes with UCPC at a sampling flow rate of 1.5 liters/min both at downstream and upstream. To provide a reliable sampling condition, the particle counter instrument (UCPC) was allowed to stabilize after switching between the two sampling ports at the downstream and upstream. Consequently the percentage penetration was measured at each tested mono-sized particle.

3.4. Filtration Efficiency Measurement

The particle penetration through the filter was determined as the ratio of the downstream concentration (C_{down}) to upstream concentration (C_{up}) for the challenge aerosol, which is presented as follow:

$$P(\%) = (\frac{C_{down}}{C_{up}}) \times 100 \qquad (3 - 2)$$

Consequently, the total collection efficiency (η) is defined as:

$$\eta(\%) = 100 - P = [1 - \frac{C_{down}}{C_{up}}] \times 100 \qquad (3 - 3)$$

As mentioned earlier, a UCPC instrument was used to count the average number concentrations at the upstream and downstream of the filter. Notes, according to the measurement technique, the total collection efficiency can be determined in terms of mass or number concentration.

3.5. Set-up Characterization (Calibration)

Prior to the filtration efficiency test, in order to provide a reliable operating conditions for the test rig and sampling procedures, some calibration and qualification tests were conducted. These calibration tests involve:

- Conducting no filter test (correlation test) to quantify the accuracy of the fractional efficiency measurement,
- Measuring the size distribution at different locations at upstream, to assure the dispersal uniformity of the challenge aerosol in the test chamber,
- Measuring the concentration and size distribution of the challenge aerosol using different NaCl solution concentrations and,
- Conducting the stabilization test during the system startup to determine the time interval until the particle concentration reaches a steady condition at upstream.

In this study, the calibration tests were implemented at four different testing constant airflow rates: 85, 135, 270 and 360 liters/min.

3.5.1. No Filter Test (Correlation Test)

The purpose of this test was to quantify the accuracy of the fractional efficiency measurement. The experiment similar to the filtration efficiency tests was conducted without any removal device (respirator). In an ideal operating condition, penetration level of 100% would be achieved at each particle size.

However, from a pragmatic perspective, a penetration lower than 100% can be expected due to the particle losses in the chamber and sampling tube measuring instruments, discrepancy in particle dispersal uniformity (mixing) between upstream and downstream sampling probes (Ensor et al., 1997).

To evaluate the mentioned criterion, the correlation ratio (R) was computed between two sampling locations at the upstream (center) and downstream at all four airflow rates: 85, 135, 270 and 360 liters/min. This correlation ratio (R) is defined as:

$$R = \left(\frac{downstream\ \ particle\ \ concentrat\,ion}{upstream\ \ particle\ \ concentrat\,ion}\right) \qquad (3-4)$$

The data analysis yielded a fairly normal deviation between the upstream and downstream concentration, satisfying the last updated requirements in the ASHRAE testing standard 52.2 (2007). The correlation ratios ranged from 0.97 to 1.09, 0.98 to 1.10, 0.93 to 1.09 and 0.92 to 1.03 with average values of 1.01, 1.06, 0.99 and 0.98 at 85, 135, 270 and 360 airflow rates, respectively (see figures 3-9 through 3-12).

The six-Jet Collision Nebulizer (operated at an inlet pressure of 35 psi and using 0.01% NaCl solution) was used to generate 6 to 200 nm poly-disperse NaCl particles.

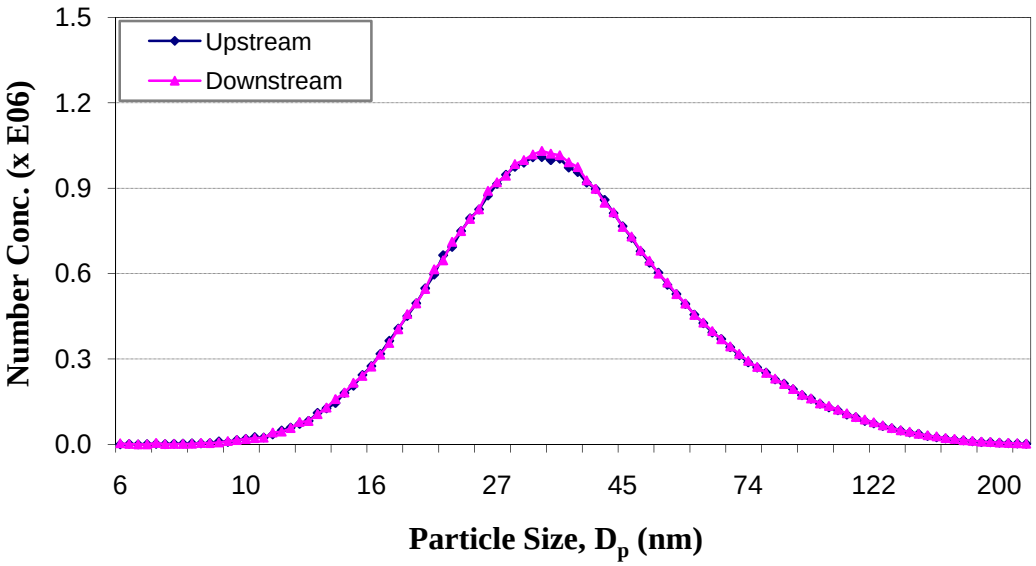

Figure 3-9: Penetration without the test filter at 85 liters/min airflow rate.

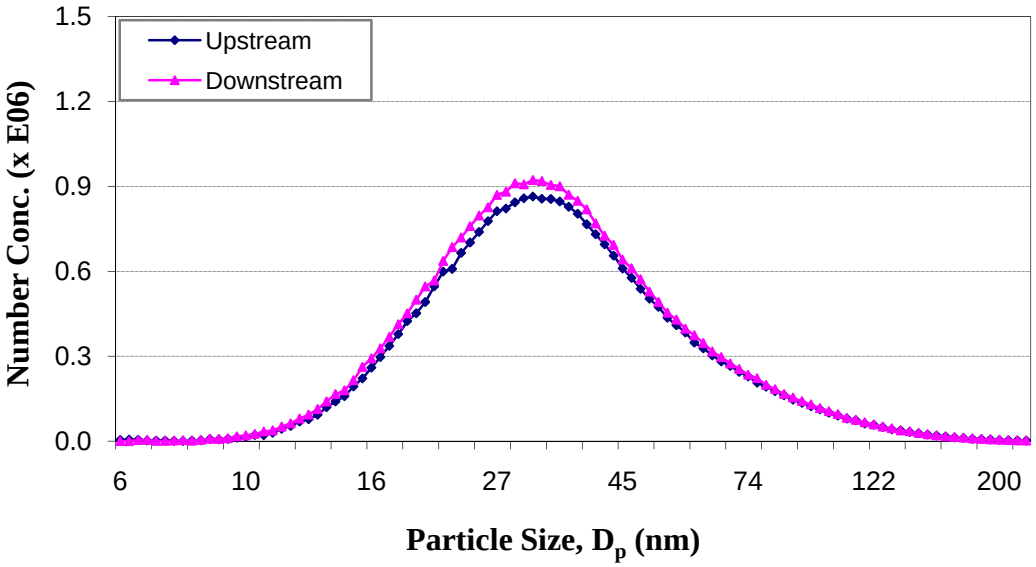

Figure 3-10: Penetration without the test filter at 135 liters/min airflow rate.

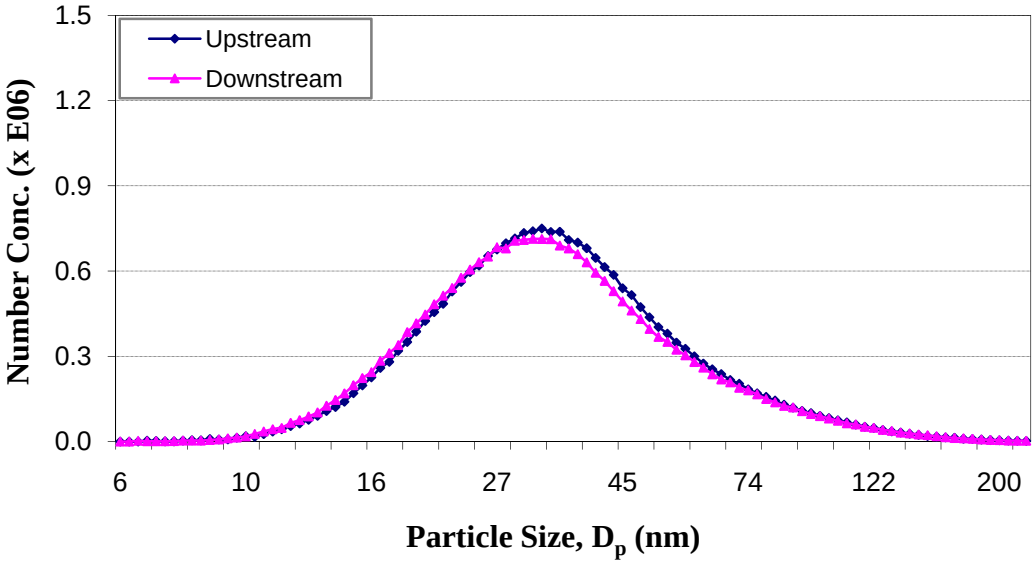

Figure 3-11: Penetration without the test filter at 270 liters/min airflow rate.

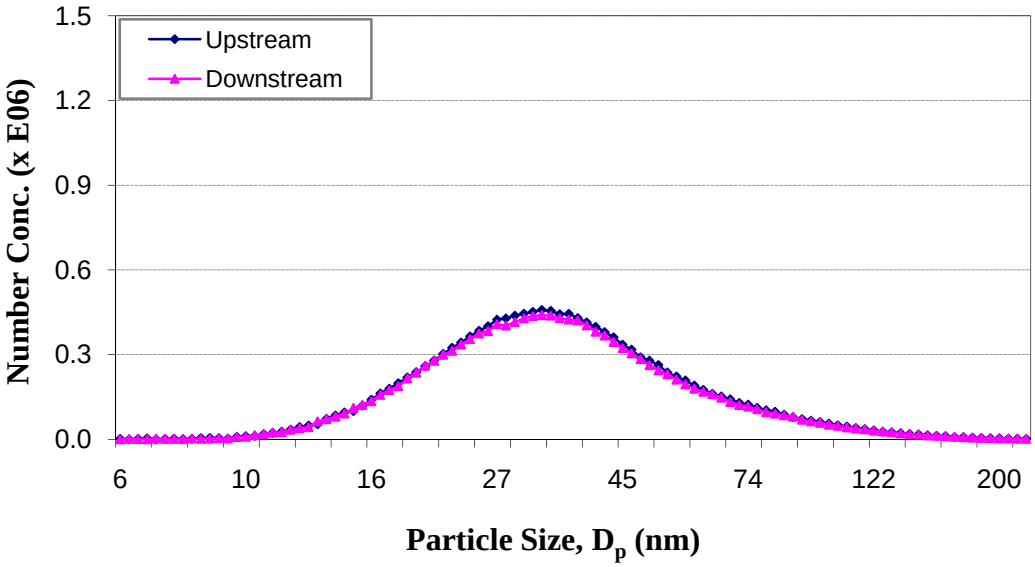

Figure 3-12: Penetration without the test filter at 360 liters/min airflow rate.

3.5.2. Particle Dispersal Uniformity Test at Upstream

This qualification test was carried out to ensure the uniformity of the particle concentration at upstream of the filter in the test chamber. To verify this, the coefficient variation (CV) of aerosol uniformity[4] was calculated at five upstream sampling locations (right up, right down, left up, left down and center) under four different airflow rates (85, 135, 270 and 360 liters/min) at each particle size, with no removal devices (see figure 3-13).

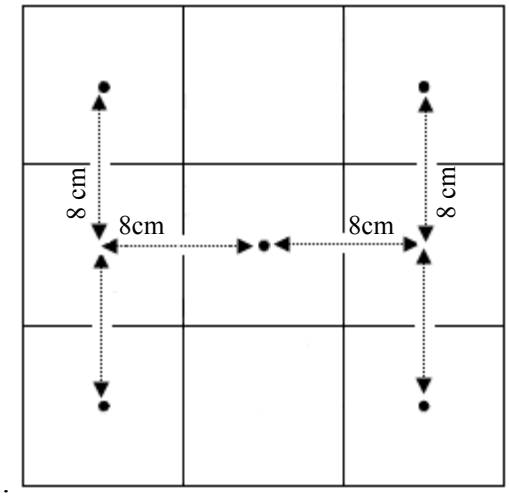

Figure 3-13: Top view of the sampling locations at upstream.

According to the data analysis for the particle size range of 6 to 200 nm, the average CV values were 4.3, 4.8, 2.8 and 5.2% at 85, 135, 270 and 360 liters/min airflow rates, respectively (see figures 3-14 through 3-17). These ranges computed for the correlation

[4] The correlation variation (CV) of aerosol uniformity is defined as the ratio of standard deviation to mean value of the particle concentration at each particle size.

variation satisfied the requirements specified in the ASHRAE testing standard 52.2 (2007) (CV < 15% for each testing airflow rate) and indicated good mixing and uniformity in the test chamber. For more detailed information, including information on the coefficient variation for the aerosol uniformity, see table 3-1.

In this experiment, the six-Jet Collision Nebulizer (operated at an inlet pressure of 35 psi and using 0.01% NaCl solution) was used to generate 6 to 200 nm poly-disperse NaCl particles.

Table 3-1: Summary of coefficient variation for the aerosol uniformity.

Airflow rate	Correlation variation (%)		
(liters/min)	Minimum	Maximum	Average
85	1.9	7.9	4.3
135	2.7	9.8	4.8
270	0.6	5.5	2.8
360	3.3	8.8	5.2

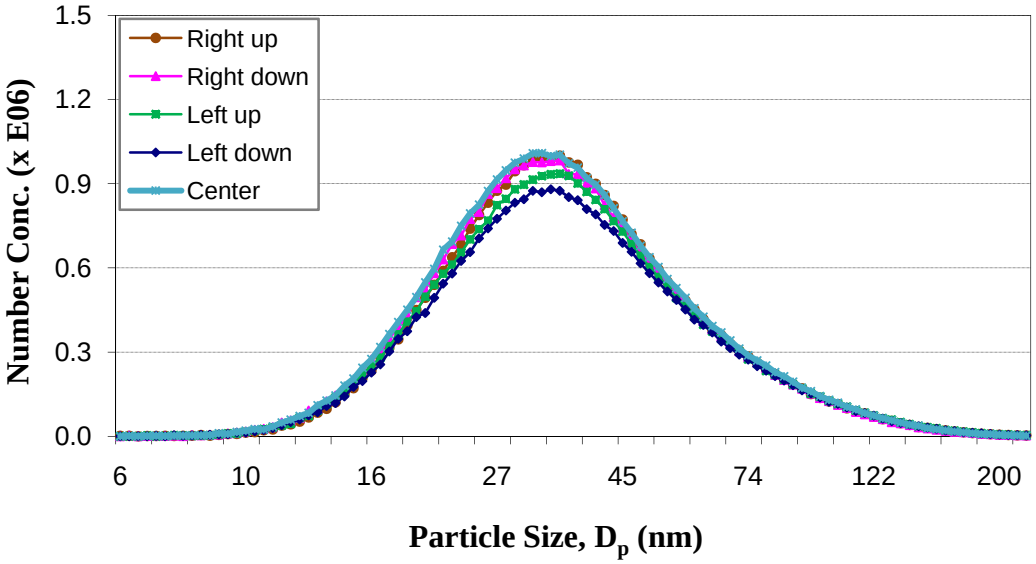

Figure 3-14: Particle size distribution at five different upstream sampling locations under 85 liters/min airflow rate.

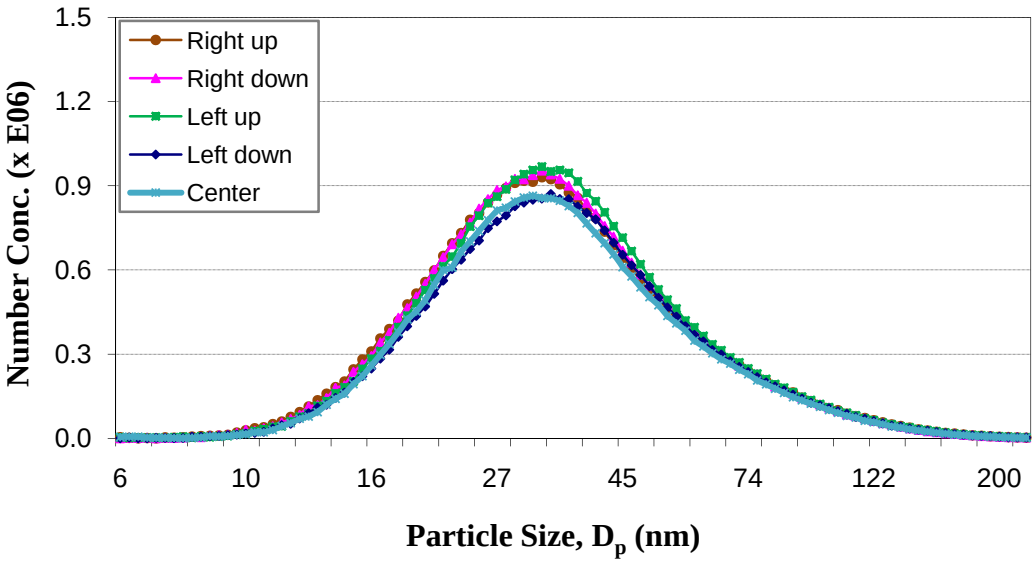

Figure 3-15: Particle size distribution at five different upstream sampling locations under 135 liters/min airflow rate.

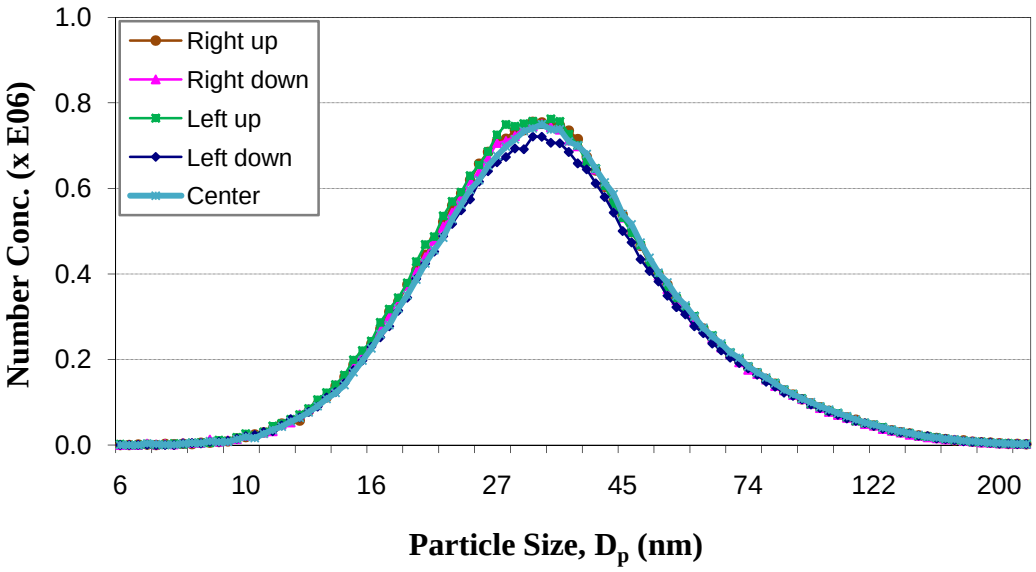

Figure 3-16: Particle size distribution at five different e upstream sampling locations under 270 liters/min airflow rate.

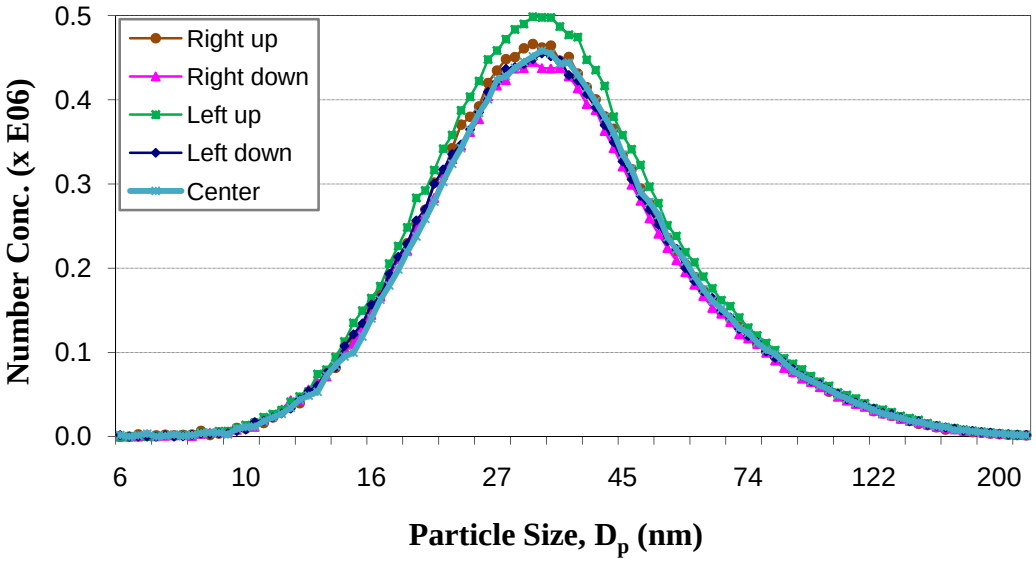

Figure 3-17: Particle size distribution at five different upstream sampling locations under 360 liters/min airflow rate.

3.5.3. Particle Size Distribution at Upstream

In this qualification test, the particle concentration and size distribution were measured at the upstream of the chamber under different airflow rates of 85, 135, 270 and 360 liters/min. The six-Jet Collision Nebulizer was used to provide particles with a size ranging between 6 to 200 nm (operated at 15, 25, 30 and 35 psi inlet pressures, using 0.01, 0.1 and 1% NaCl solution concentrations). Like the other previous qualification tests, the experiment was conducted without a respirator on the manikin.

According to the obtained results, at the same inlet pressure, with an increase in salt solution concentration (used to generate poly-disperse particles) the particle number concentration was found to increase at each particle diameter (see figures 3-18 through 3-20). The particle size distribution also demonstrated a shift toward larger sizes. For instance, when operating the Nebulizer at 35 psi and 85 liters/min airflow rate, the maximum particle concentrations were 1.0E06, 1.65E06 and 2.63E06 particles/cm^3 at 34, 50 and 70 nm in size using 0.01, 0.1 and 1% NaCl solutions, respectively (see figures 3-18 through 3-20).

In addition, with increased inlet pressures, the particle concentration was found to elevate at each particle size. For instance, using 0.01% NaCl solution, at 85 liters/min airflow rate, the maximum particle concentrations were approximately 0.25E06, 0.58E06, 0.78E06 and 1.0 E06 particles/cm^3 at 15, 25, 30 and 35 psi, respectively (see figure 3-18).

A similar pattern was also observed for the particle concentration and size distribution at higher airflow rates of 135, 270 and 360 liters/min at upstream, except for lower concentration due to increased airflow (see appendix D).

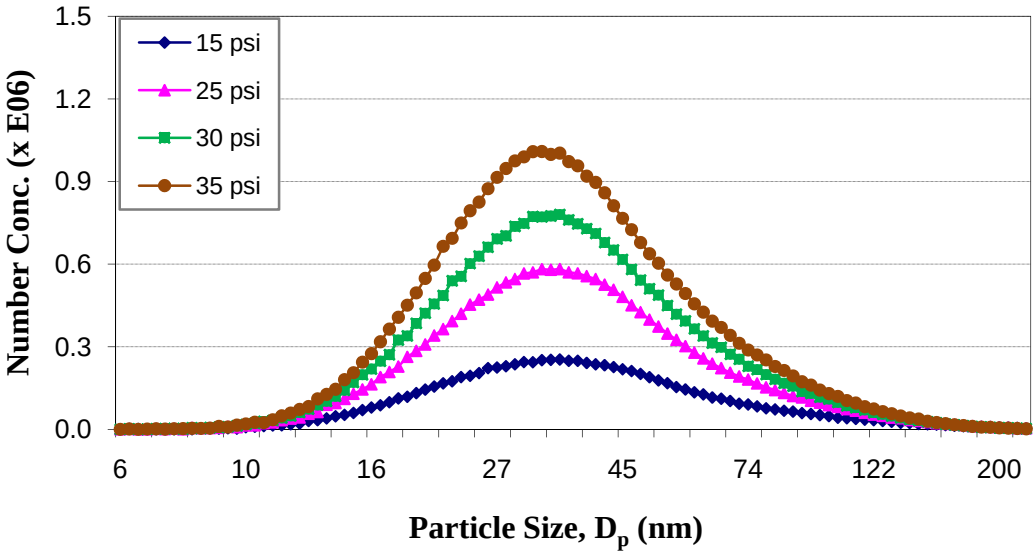

Figure 3-18: Particle concentration as a function of particle size at different pressures (85 liters/min and 0.01% NaCl solution).

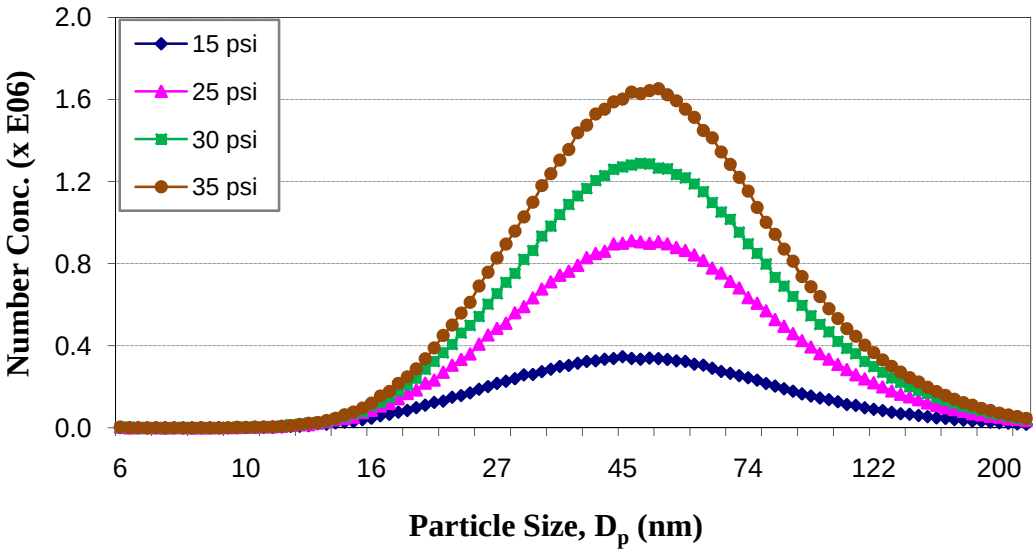

Figure 3-19: Particle concentration as a function of particle size at different pressures (85 liters/min and 0.1% NaCl solution).

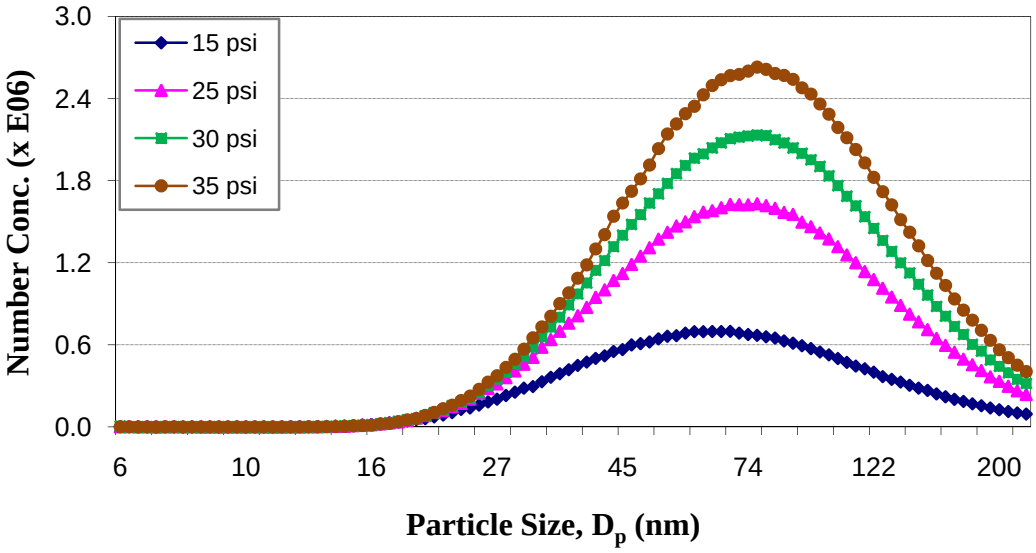

Figure 3-20: Particle concentration as a function of particle size at different pressures (85 liters/min and 1% NaCl solution).

3.5.4. Stabilization Test

A stabilization test was conducted at four different constant airflow rates (85, 135, 270 and 360 liters/min) to determine the time interval required for the particles to reach a steady state concentration. The six-Jet Collision Nebulizer was operated at 35 psi inlet pressure to generate poly-disperse NaCl particles, using 0.01% NaCl solution.

The preferred stabilization times were 1.95, 1.35, 0.82 and 0.57 minutes at 85, 135, 270 and 360 liters/min airflow rates, respectively (see table 3-2). According to the data analysis, after the set-up was stabilized, the total number concentrations for the generated poly-disperse aerosols were approximately 0.63E06, 0.54E06, 0.40E06 and 0.32E06 particles/cm^3 at the respective airflow rates.

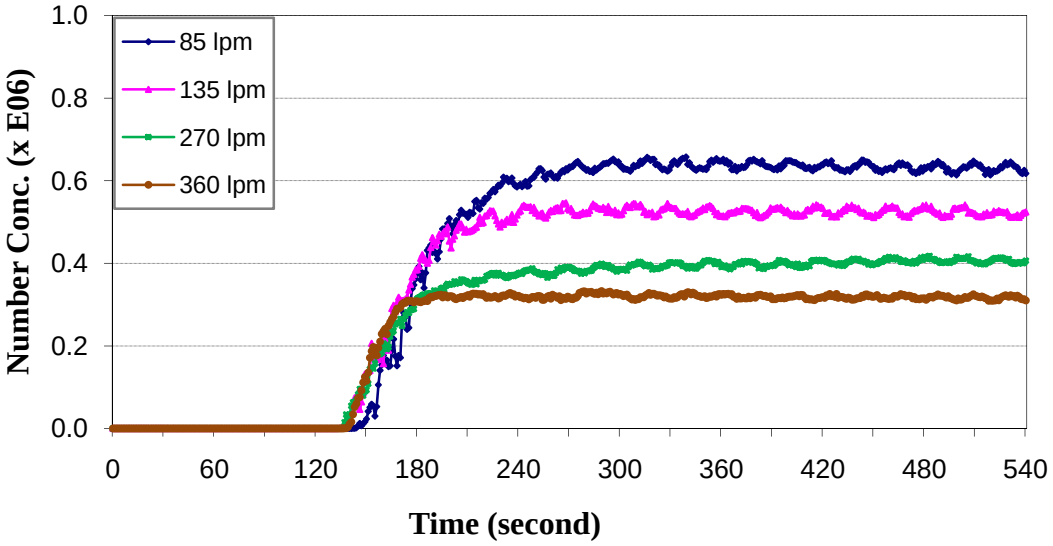

Figure 3-21: Challenge aerosol concentration during system startup at different airflow rates, using 0.01% NaCl.

In addition, as noticed in figure 3-21, some inconsistency occurred in the particle number concentration even after the stabilization period. This fluctuation occurred in a cycle nearly at every 20 seconds. However, no explanation was found for this phenomenon. Table 3-2 presents a summarized result for the stabilization test at all four testing airflow rates.

Table 3-2: Summary of stabilization test.

Airflow rate (liters/min)	Stabilization time (min)	Particle concentration (xE06 particles/cm^3)
85	1.95	0.63±0.01
135	1.35	0.54±0.01
270	0.82	0.40±0.02
360	0.57	0.32±0.06

Chapter 4: RESULTS AND DISCUSSION

4.1. Introduction

The proposed research was carried out for two sets of experiments. In the first set-up, an experimental methodology has been developed to test N95 respirators against 15 to 200 nm poly-disperse aerosols in three different scenarios (see figure 3-2). First, the effect of airflow condition (85, 135, 270 and 360 liters/min) and particle size on the initial penetration and the quality factor levels of the N95 respirator were investigated. Thereafter, the effect of particle loading on the filtration performance of the N95 respirator was examined at constant airflow rate of 85 liters/min. Finally, the correlation between relative humidity (RH) and initial percentage penetration was assessed at 85 liters/min constant airflow rate.

In the second phase, the experimental set-up was adapted to test N95 respirators against mono-disperse particles (at twelve particle sizes) with a size range of 20 to 200 nm at constant airflow rate of 85 liters/min (see figure 3-1). The results have also been correlated with the initial particle penetration values measured at constant airflow rate of 85 liters/min when challenged with poly-disperse aerosols.

In this chapter, the outcomes of each experiment are explained and discussed in details.

4.2. PHASE 1: Particle Penetration against NaCl Poly-Disperse Particles in the Range 15 to 200 nm (PAT Method)

4.2.1. Initial Particle Penetration as a Function of Inhalation Flow Rate

Test Description

The N95 respirators were challenged with poly-disperse NaCl aerosols for a period of 5 minutes at four constant airflow rates: 85, 135, 270 and 360 liters/min. The experimental set-up was developed to test filters against poly-disperse aerosols (see figure 3-2).

Data Analysis

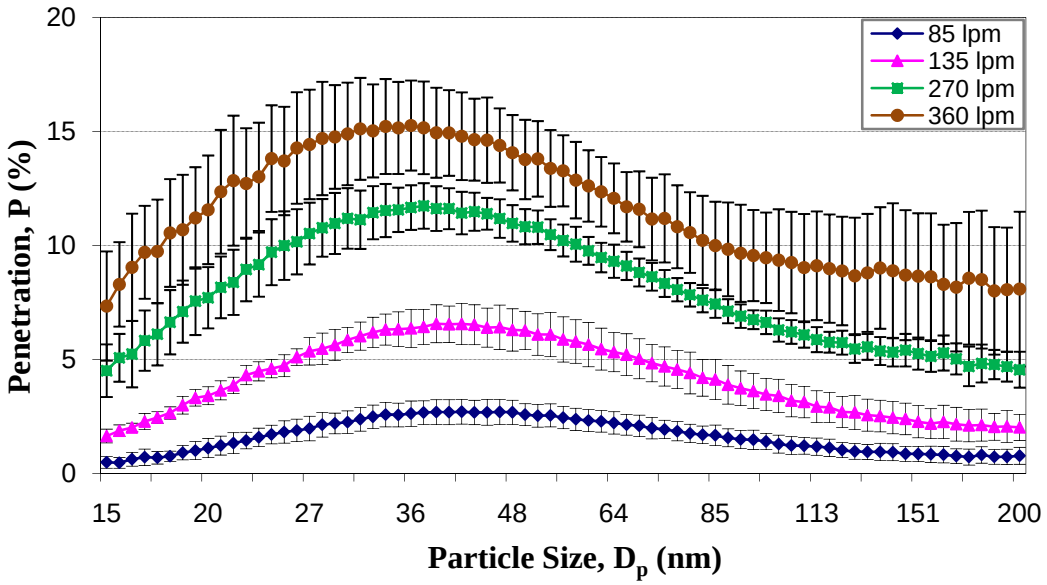

Figure 4-1: Effect of particle size and inhalation flow rate on initial particle penetration through N95 respirators (n=3). The error bars represent the standard deviations.

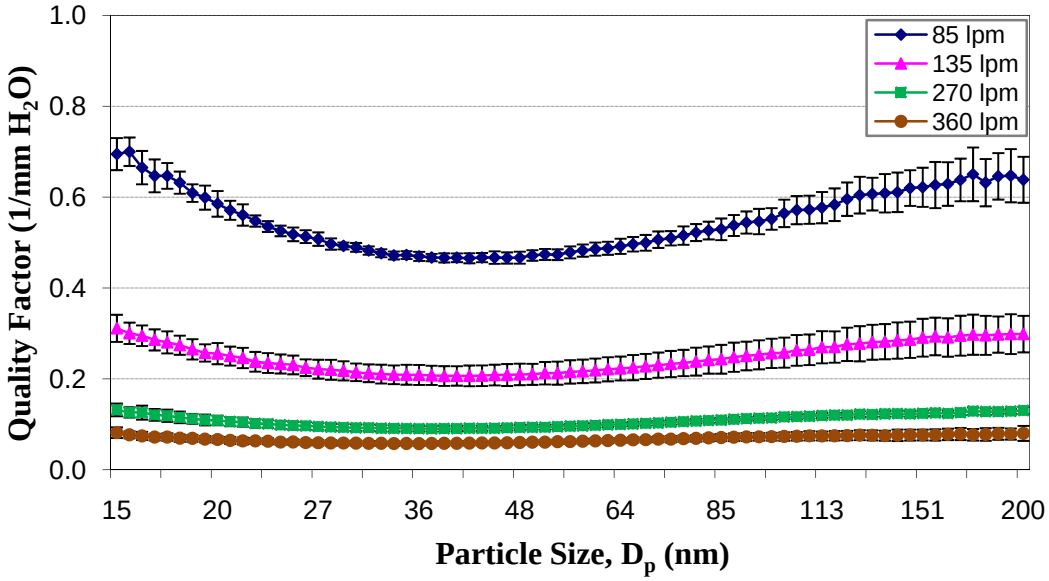

Figure 4-2: Effect of particle size and inhalation flow rate on filter quality factor of N95 respirators (n=3). The error bars represent the standard deviations.

Figure 4-1 demonstrates the initial particle penetration values through N95 respirators at four constant airflow rates when challenged with 15 to 200 nm poly-disperse sodium chloride aerosols. The test was repeated three times for an identical N95 respirator model. The mean, peak and standard deviation of initial penetration values were computed at each particle diameter with respect to the airflow rate.

Consistent with the results from the previous studies, the initial particle penetration was significantly enhanced as the airflow rate increased (Balazy et al., 2006a, 2006b; Richardson et al., 2006; Huang et al., 2007; Kim et al., 2007; ; Eninger et al., 2008). As anticipated, the maximum initial penetration level through N95 respirators dramatically exceeded 5% NIOSH certification criterion at about 1.30, 2.35 and 3.05 folds at high airflow rates of 135, 270 and 360 liters/min, resepectively. At the Most Penetrating

Particle Sizes (MPPS), with the lowest filtration efficiency, the percentage penetrations were 2.7±0.54, 6.6±0.90, 11.7±1.00 and 15.3±1.97% at 85, 135, 270 and 360 liters/min, repectively. The mean initial penetrations were also 1.64±0.72, 4.21±1.60, 8.13±2.43 and 11.46±2.51% at the respective airflow rates for the tested particle size range of 15 to 200 nm.

However, compared with the obtained results for the particle size range from 15 to 200 nm, the data analysis suggested higher mean initial penetrations for the particle size range <100 nm; 1.89±0.67, 4.82±1.40, 9.13±2.03 and 12.45±2.16% at 85, 135, 270 and 360 liters/min airflow rates, respectively (see table 4-1). Meanwhile, the coefficient variation for the initial penetration was altered from 0.19 to 0.53, 0.07 to 0.22, 0.06 to 0.28 and 0.11 to 0.33 at the respective airflow rates.

The mean initial particle penetration at 360 liters/min exceeded that at 85 liters/min by about 7-fold. In addition, according to the obtained results, with the increase of airflow rate, the MPPS demonstrated a shift toward small particles; approximately 46, 41, 37 and 36 nm at 85, 135, 270 and 360 liters/min, respectively, which was consistent with the literature (Martin and Moyer, 2000; Balazy et al., 2006a, 2006b; Richardson et al., 2006; Huang et al., 2007; Rengasamy et al., 2008a; Rengasamy and Shaffer, 2008b). The shift in MPPS toward small sizes and the increase in the particle penetration are both due to the fact that, along with the increase in airflow rate, the diffusion and electrostatic mechanisms contribute less to the removal of smaller particles as a result of less residence time (Richardson et al., 2006).

It should be noted that NIOSH certifies the N95 filtering face-piece respirators based on filtration efficiency higher than 95% at the MPPS of 300 nm (CFR, 1996). However, as observed in figure 4-1, the initial penetration in the MPPS occurred at a particle size smaller than 300 nm at all airflow rates. Some previous studies reported that the iso-propanol treatment (applied to remove the electrostatic charge) of N, R and P types would shift the MPPS from 30- 100 nm to 250- 350 nm and the particle penetration levels would increase significantly, confirming that the electrostatic mechanism plays a significant role in the filtration performance for N and P type respirators (Martin and Moyer, 2000; Huang et al., 2007; Rengasamy et al., 2007).

Furthermore, along with increasing the airflow rate, the quality factor value was reduced, while not significantly dependent upon the particle size (see figure 4-2). This dramatic drop in the quality factor values, particularly at higher airflow rates, is largely attributed to the increase in the pressure drop and particle penetration, which is in agreement with the literature (Han, 2000; Eninger et al., 2008).

According to the results, more enhanced values were observed for the quality factor at low airflow rates (85 and 135 liters/min), which was improved by average factors of 8.1 at 85 liters/min and 3.6 at 135 liters/min compared with that at 360 liters/min. Conversely, the quality factors were considerably low and roughly identical at 270 and 360 liters/min. As seen in table 4-1, the mean quality factors for the particles between 15 to 200 nm were 0.548±0.067, 0.247±0.032, 0.108±0.013 and 0.068±0.007 at 85, 135, 270 and 360 liters/min airflow rates, respectively. In comparison with the results obtained for the particles between 15 to 200 nm in size, the data analysis suggested a similar mean

quality factor for the particles below 100 nm in size; 0.5248±0.062, 0.2342±0.026, 0.102±0.011 and 0.065±0.006 at the respective airflow rates (see table 4-1).

Table 4-1: Summary of particle penetration, pressure drop, quality factor and coefficient of variation for the particle penetration.

Q	Pressure drop	Maximum P (15-200 nm)	MPPS (15-200 nm)	P15-200 nm	Qf 15-200 nm	P15-100 nm	Qf 15-100 nm	CV* (15-200 nm)	CV* (15-100 nm)
(liters/min)	(mm H20)	(%)	(nm)	(%)	(1/ mm H2O)	(%)	(1/ mm H2O)	(%)	(%)
85	7.79±0.27	2.7±0.54	46	1.64±0.72	0.548±0.067	1.89±0.67	0.5248±0.062	0.19-0.53	0.19-0.53
135	13.32±1.03	6.6±0.90	41	4.21±1.60	0.247±0.032	4.82±1.40	0.2342±0.026	0.07-0.34	0.07-0.22
270	23.79±0.77	11.7±1.00	37	8.13±2.43	0.108±0.013	9.13±2.03	0.102±0.011	0.06-0.28	0.06-0.28
360	32.71±0.91	15.3±1.97	36	11.46±2.51	0.068±0.007	12.45±2.16	0.065±0.006	0.11-0.42	0.11-0.33

*Coefficient of variation is defined as the ratio of standard deviation to the mean.

4.2.2. Particle Penetration as a Function of Loading Time

Test Description

The selected N95 respirator was loaded continuously against 15 to 200 nm poly-disperse NaCl particles at 85 liters/min constant airflow rate for a time interval of 5 hours. The experimental methodology was developed to test filters against poly-disperse aerosols (see figure 3-2).

Data Analysis

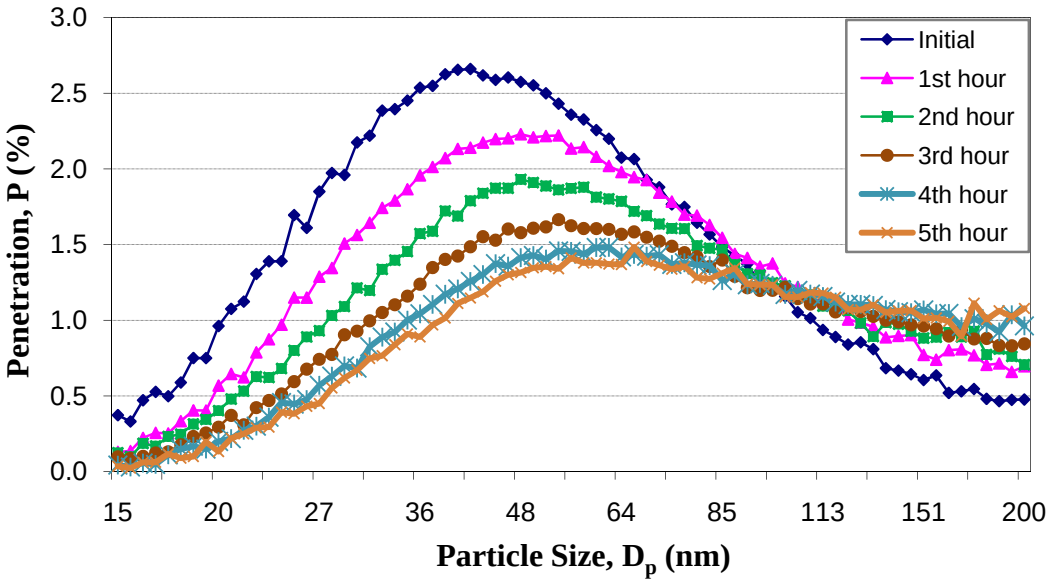

Figure 4-3: Effect of particle loading on particle penetration through N95 respirators at 85 liter/min constant airflow rate (n=3).

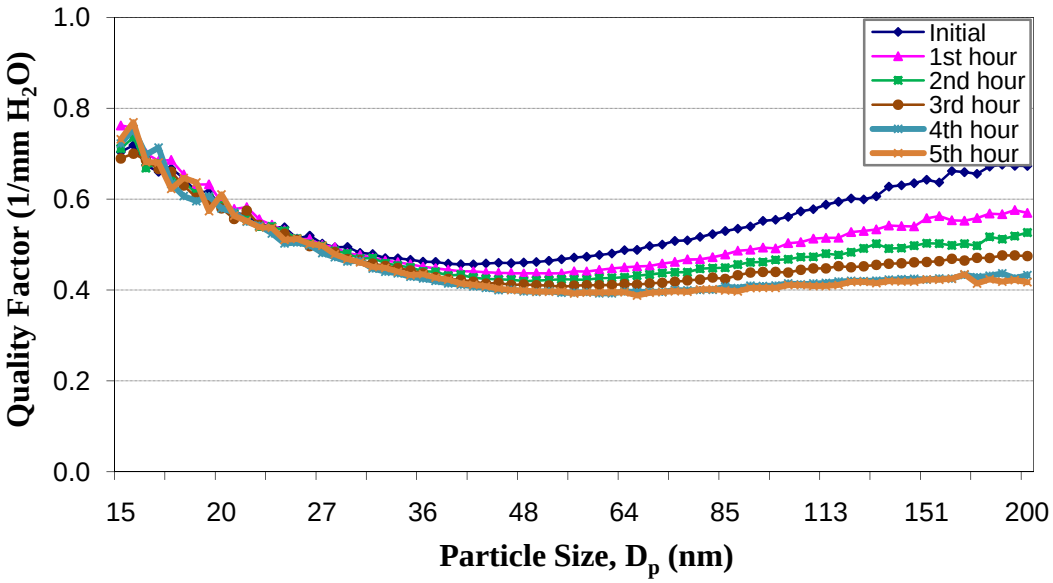

Figure 4-4: Effect of particle size and particle loading on filter quality factor of N95 respirator at 85 liters/min constant airflow (n=3).

Figure 4-3 illustrates the effect of particle loading on the particle penetration level through the N95 respirator at constant airflow rate of 85 liters/min against poly-disperse sodium chloride particles. The test was replicated three times for an identical N95 respirator model. The mean, peak particle penetrations and also the quality factor for the N95 respirator were determined over time (once at each hour).

For the particles below 100 nm in size, the penetration level was found to diminish with further particle loading. Conversely, the results demonstrated that for the particles roughly larger than 100 nm, the penetration increases over loading time. As summarized in table 4-2, for the particles below 100 nm, the maximum and mean penetration levels were reduced from 2.66±0.21 to 1.48±0.12% and from 1.76±0.70 to 0.87±0.50%,

respectively. Meanwhile, an increase in the mean penetration level from 0.71±0.21 to 1.07±0.07% (see table 4-2) was observed for the larger particles.

It was recognized that the MPPS for the N95 respirator shifted toward the large particle sizes; from 41 to 66 nm. This is because diffusion becomes more dominant to collect NPs while electrostatic attraction force shows less contribution in capturing large size particles (Martin and Moyer, 2000, Wang, 2001; Woon et al., 2008). Moreover, less deviation in particle penetration was identified with further particle loading (see figure 4-3).

As mentioned earlier in the section, the penetration for the particles between 15 to 100 nm showed a considerable reduction with the loading process, whereas, the penetration gradually increased for the larger sizes. Seemingly, this phenomenon is due to the formation of particle dendrites on the surface of the filter (Wang, 2001; Woon et al., 2008). With the lack of electrostatic attraction force, particle loading generally leads to an increase in capturing the particles, as the deposited particles are similar in size to the approaching particles. This allows the particles to remain straight in their gas stream lines adjacent to the fiber surface (Wang, 2001). On the contrary, the captured particles may suppress the collection of particles caused by the electrostatic attraction force, which is a noticeable collection mechanism for the large size particles predominantly between 150 to 500 nm (Wang, 2001). Experimental studies on electret filters verified that the particle collection efficiency relies generally on the amount of electrostatic charge on the filter fiber (Brown et al., 1988; Chen et al., 1993; Martin and Moyer, 2000).

Figure 4-4 displays the filter quality pattern of the N95 respirator at each particle diameter during the filter loading. The results showed further discrepancy in the quality factors at larger particle sizes (the quality factor values were similar at very nano-sized particles over the aerosol loading time). As shown in table 4-2, for the particles between 15 to 200 nm, the mean quality factor value differed from 0.551±0.077 to 0.457±0.088 in the early and late stages of the filter loading, respectively. The quality factors for the particles below 100 nm also changed between 0.507±0.086 to 0.471±0.099 in the respective stages.

Table 4-2: Summary of particle penetration, pressure drop and quality factor in the early (A) and late (B) stages of particle loading.

Q	Particle loading stage	Pressure drop	Maximum P (15-200 nm)	MPPS (15-200 nm)	P15-200 nm	P15-100 nm	P100-200 nm	Qf 15-200 nm	Qf 15-100 nm
(liters/min)		(mm H20)	(%)	(nm)	(%)	(%)	(%)	(1/ mm H2O)	(1/ mm H2O)
85	(A)	7.95±0.57	2.66±0.21	41	1.48±0.77	1.76±0.70	0.71±0.21	0.551±0.077	0.507±0.086
85	(B)	10.86±1.27	1.48±0.12	66	0.92±0.44	0.87±0.50	1.07±0.07	0.457±0.088	0.471±0.099

4.2.3. Particle Penetration as a Function of Relative Humidity (RH)

Test Description

The respirator was tested against 15 to 200 nm poly-disperse NaCl particles at constant airflow rate of 85 liters/min at three relative humidities; 10, 30 and 70% for 5 minutes. A similar experimental methodology was established to perform the filtration efficiency tests against poly-disperse aerosols (see figure 3-2), except a MNR humidifier was utilized to condition the relative humidity before the total air entered the inlet chamber.

Data Analysis

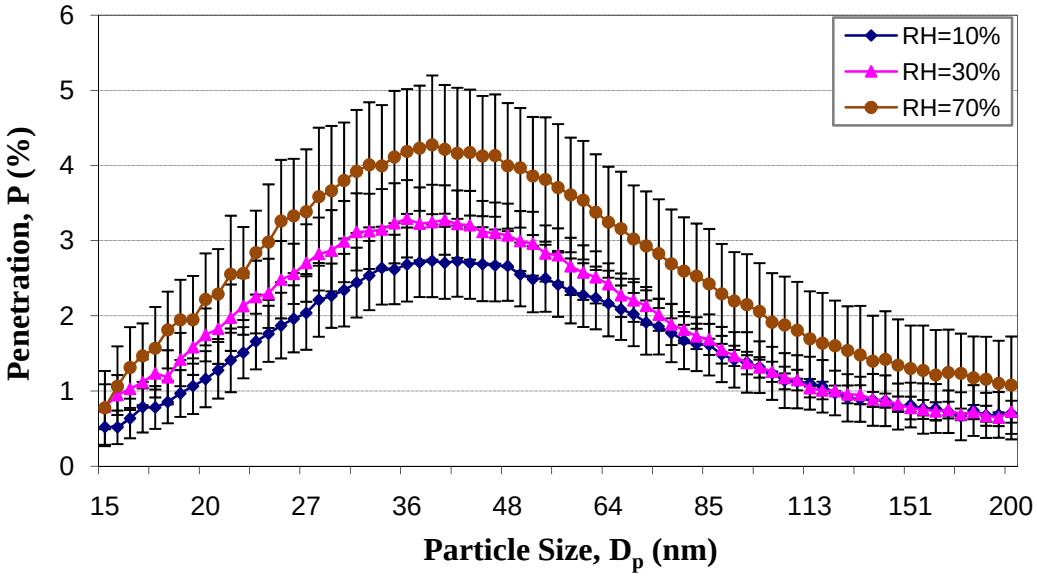

Figure 4-5: Effect of relative humidity on initial particle penetration through N95 respirators at 85 liters/min constant airflow rate (n=4). The error bars represent the standard deviation at each point.

Figure 4-5 presents the initial penetration of sodium chloride particles through the selected N95 respirators at Q=85 liters/min at three different relative humidities (10, 30 and 70%). The test was replicated four times for the selected N95 respirator model at each relative humidity for the particles ranging from 15 to 200 nm. The mean, peak and standard deviation of initial penetration levels were determined. Consistentent with the results obtained from the previous studies on electret filters, for the particles below 100 nm, with an increase of the (RH), lower filtration performance was observed steadily, and is attributed to the reduction in the charges on the fiber filters and particles (Ackley, 1982; Moyer et al., 1989). However, for the large sized particles, the particle penetration levels were first similar at 10 and 30% (RH); whereas subsequently increased as (RH) elevated to 70% (see figure 4-5).

As expected, the maximum initial penetration was found to escalate as the (RH) increased, but, in all cases not exceeded up to 5% NIOSH certification criterion. In this regard, the penetrations in the MPPS were respectively 2.73±0.47, 3.30±0.50 and 4.27±0.90% at 10, 30 and 70% (RH). The penetration mean values were 1.6±0.73, 1.9±0.90, 2.6±1.10% at the respective (RH) for the particles ranging in size from 15 to 200 nm.

It is noteworthy that the filtration data displays more mean penetrations for the particles below 100 in size; 1.9±0.66, 2.3±0.75 and 3.0±0.94% at 10, 30 and 70% (RH), respectively (see table 4-3).

The initial particle penetration exceeded by an average factor of 1.6 at the relative humidity of 70%. With an increase in (RH), at the MPPS, no consistent shift was

identified. However, the MPPS still occurred in the nano-sized range between 30 to 50 nm, acknowledging the presence of electrostatic attraction on the collection of particles (see table 4-3). For more detailed information including the data analysis on the initial penetrations, MPPS and coefficient variation of the particle penetration, review table 4-3.

Table 4-3: Summary of particle penetration for the respirator's

Q	(RH)	Maximum P (15-200 nm)	MPPS (15-200 nm)	P15-200 nm	P15-100 nm	CV* (15-200 nm)	CV* (15-100 nm)
(liters/min)	(%)	(%)	(nm)	(%)	(%)	(%)	(%)
85	10	2.73±0.47	41	1.6±0.73	1.9±0.66	0.17-0.73	0.17-0.66
85	30	3.30±0.50	36	1.9±0.90	2.3±0.75	0.07-0.90	0.09-0.75
85	70	4.27±0.90	39	2.6±1.10	3.0±0.94	0.19-1.09	0.19-0.94

* Coefficient of variation is defined as the ratio of standard deviation to the mean.

4.3. PHASE 2: Particle Penetration against NaCl Mono- Disperse Particles in the Range 20 to 200 nm (MAT Method)

4.3.1. Correlation of Mono-Disperse and Poly-Disperse Particle Penetration

Test Description

The filtration performance of N95 series respirators was investigated against twelve different mono-sized NaCl particles (20, 30, 40, 45, 50, 55, 60, 80, 100, 120, 160 and 200 nm) at 85 liters/min constant airflow rate. An experimental method was developed to test filters against mono-disperse aerosols (see figure 3-1).

Data Analysis

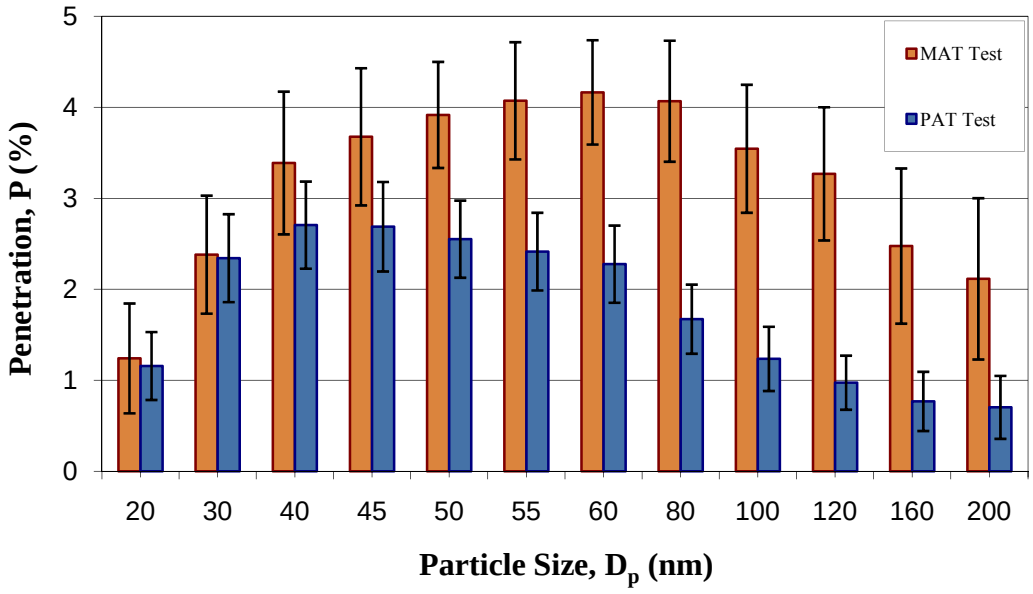

Figure 4-6: The comparison of mono-disperse and poly-disperse particle penetration levels (n=4). The error bars represent the standard deviation at each point.

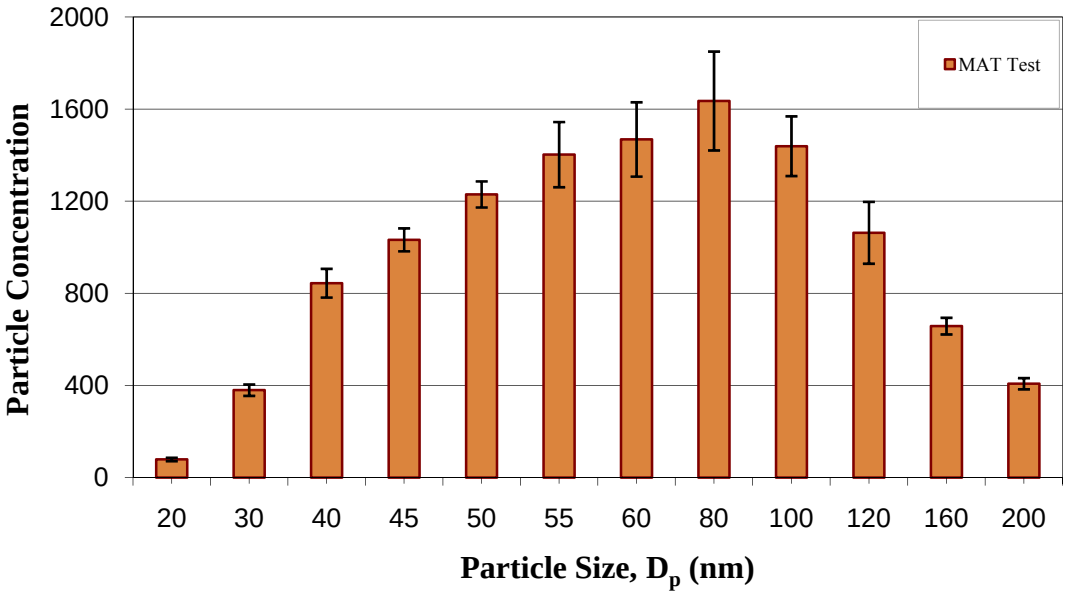

Figure 4-7: The particle number concentration at each tested mono-sized particle (n=4). The error bars represent the standard deviation at each point.

Figure 4-6 illustrates the particle penetration levels through N95 respirators at constant airflow rate of 85 liters/min against mono-disperse sodium chloride particles using the mono-disperse aerosol test (MAT) method. It also shows the results with the measured penetrations at constant airflow rate of 85 liters/min when challenged with poly-disperse aerosols. The test was repeated with four identical N95 respirators model against mono-sized NaCl aerosols. Consistent with the results from the previous studies for the electret filters, the MPPS occurred in the 40 to 100 nm range. Compared with the obtained results when N95 respirator was challened against poly-disperse aerosols test (PAT) method, higher initial penetration level was found at each tested particle size with the (MAT) method (see figure 4-6). However, in all cases, the initial penetration never exceeded the 5% NIOSH certification criterion at 85 liter/min.

The results also revealed no significant relation between the initial particle penetrations, measured with (MAT) and (PAT) methods at each corresponding particle size at 85 liters/min.

In addition, as observed in figure 4-7, the results showed very low number concentration of nano-particles at the upstream of the N95 respirator compared with the measured number concentratin with (PAT) method at each corresponding particle size at 85 liters/min. Depending on the particle size, the number concentration were approximately between 80 to 1600 particles/cm^3. This low number concentration of nano-particles is mainly due to the diffusion losses through the measuring instrument; Scanning Mobility Particle Sizer (SMPS), mainly from five parts: the penetration through the impactor inlet, penetration through the neutralizer, penetration through the tubing to the Differential Mobility Analyzer (DMA) and CPC, penetration through the DMA and penetration through the CPC (review the TSI manual for series 3080 electrostatic classifiers).

.

Chapter 5: CONCLUSIONS AND FUTURE WORK

5.1. Conclusions

The main objective of this research was to develop a methodology to characterize the effectiveness of one model of NIOSH-approved N95 respirator against poly-disperse aerosols in size range from 15 to 200 nm. Then to use this methodology 1) to investigate the effect of airflow condition and particle size on the initial particle penetration through the respirator, 2) to investigate the effect of two other parameters, such the time of use and the relative humidity on filtration performance, and 3) to develop and adapt the experimental set-up to challenge the same type of respirator against mono-disperse particles with a size range between 20 to 200 nm.

In order to achieve the objective of the study, an experimental set-up was first designed, constructed and calibrated for testing filters for capturing NPs. A methodology was developed to generate a controlled atmosphere of NPs, and to characterize the particles (in terms of size and number distribution) and measure the concentration of the NPs in an enclosed system. Then, a methodology was developed to characterize the performance of filters used for respiratory protections in different scenarios, for capturing the NPs.

The conclusions of this study are as follow:

- Challenging N95 respirators with poly-disperse aerosols, the initial particle penetration was dramatically enhanced with an increase in airflow rate. The initial penetration in the MPPS through N95 respirator dramatically exceeded 5%

NIOSH certification criterion by average factors of 1.30, 2.35 and 3.05 at high airflow rates of 135, 270 and 360 liters/min, respectively. The MPPS was shifted toward small particle size; approximately 46, 41, 37 and 36 nm at 85, 135, 270 and 360 liters/min, respectively.

- The particle penetration level through N95 respirator reduced for the particle size range nearly below 100 nm at 85 liters/min airflow rate with further particle loading, while, a gradual increase in particle penetration was observed for the larger size particles. The MPPS was also found to shift toward the large particle sizes; from 41 to 66 nm.

- For the particles nearly below 100 nm, the filtration performance was reduced as the relative humidity increased. However, the filtration performance was similar at (RH) of 10 and 30%; and subsequently increased as (RH) elevated to 70%. The MPPS was not significantly affected by (RH).

- It was found that when challenging N95 respirators against mono-disperse aerosols using (MAT) method, the initial particle penetration never exceeded <5% NIOSH certification criterion. The MPPS also occurred in the 40 to 100 nm range. However, no consistent correlation was found for the measured initial particle penetrations with those obtained using poly-disperse aerosols test (PAT) method.

5.2. Recommendations and Future Work

The recommendations for the future research work on filtration performance assessments are as follow:

- The developed methodology has the ability to investigate the collection efficiency of series of filtering face-piece respirators. Thus, it is recommended to test three classes of N, R and P respirators with three levels of filter efficiency; 95, 99 and 99.97%, for each class of filters against solid and liquid particles. Due to the conditions aforementioned, N type of respirators correspond to the filters with resistance against only solid aerosol (not efficient against oily aerosols), while the R and P type respirators are also intended to be fairly and highly resistant, respectively, against oily aerosols.

- The method should be modified such that more reliable to challenge filtering face-piece respirators against mono-disperse particles. As mentioned before, when respirators were challenged with MAT method, low concentration was obtained at each tested particle size at the upstream of the filter compared with that achieved with PAT method.

- The method should be applicable to investigate the performance of respiratory mask filters under a realistic airflow pattern (cyclic airflow). Previous studies were almost limited to test filters at constant airflow rates. However, the results of these studies cannot be inferred for real applications because a realistic airflow rate through a respiratory mask filter is not constant and varies corresponding to

breathing rate. It is suggested that the performance of a filter under a periodic airflow rate would be different than that of measured under constant airflow rate.

- Last but not least, improved guidance in the selection and use of respirators against nano-particles should be developed to ensure high levels of respiratory protection for workers and exposed persons.

REFRENCES

Ackley, M.W. (1982). *Degradation of Electrostatic Filters at Elevated Temperature and Humidity.* 3rd World Filtration Congress pp. 169–176.

Alonso, M., Kousaka, Y., Hashimoto, T., & Hashimoto, N. (1997). *Penetration of Nanometer-Sized Aerosol Particles through Wire Screen and Laminar Flow Tube.* Journal of Aerosol Science, 27, 471–480.

ASHRAE. Standard 52.2. (2007). *Method of Testing General Ventilation Air-Cleaning Devices for Removal Efficiency by Particle Size.* American Society of Heating, Refrigerating, and Air-Conditioning Engineers, Inc., Atlanta.

Balazy, A., Podgorski, A., & Gradon, L. (2004). *Filtration of Nano-sized Aerosol Particles in Fibrous Filters. I- Experimental Results.* Journal of Aerosol Science, 35, 967–968.

Balazy, A., Toivola, M., Adhikari, A., Sivasubramani, S.K., Reponen, T., & Grinshpun, S.A. (2006a). *Do N95 Respirators Provide 95% Protection Level against Airborne Viruses, and How Adequate Are Surgical Masks?.* American Journal of Infection Control, 34, 51–57.

Balazy, A., Toivola M., Repoen T., Podgorski A., Zimmer A., & Grinshpun S.A. (2006b). *Manikin-Based Performance Evaluation of N95 Filtering Face-Piece Respirators Challenged with Nano-particles.* Annals of Occupational Hygiene, 50, 259–269.

Baumgartner, H., Loffler, F., & Umhauer, H. (1986). *Deep-Bed Electret Filters-The Determination of Single Fbre Charge and Collection Efficiency.* IEEE Transactions on Electrical Insulation, 21, 477–486.

BGI. (2002). *Collision Nebulizer-Instructions. MRE 1, 3, 6 and 24 Jet.* BGI Incorporated.

Boskovica, L., Agranovskia, I.E., Altmana, I.S., & Braddocka, R.D. (2008). *Filter Efficiency as a Function of Nano-Particle Velocity and Shape.* Journal of Aerosol Science, 39, 635–644.

Brown, R.C. (1993). *Air Filtration: An Integrated Approach to the Theory and Applications of Fibrous Filters.* Oxford U.K.: Pergamon.

Chen, C.C., Lehtimäki, M., & Willeke, K. (1993). *Loading and filtration characteristics of filtering facepieces.* American Industrial Hygiene Association Journal 54:2, 51–60.

Chen, C.C., & Huang, S.H. (1998). *The Effect of Particle Charge on the Performance of a Filtering Face-Piece.* American Industrial Hygiene Association Journal, 59, 227–233.

Code of Federal Regulations (CFR). (1996). *Approval of Respiratory Protective Devices.* Title 42, Part 84, pp. 528–593.

Crooks, M. (2007). *Nano-Safty and Instrumentation.* NanoMicroClub Networking Event. Presented by Crooks (TSI Inc.) 22nd May on Oxford.

Davies, C.N. (1973). *Air Filtration.* Academic Press, London.

De la Mora, J. F., De Juan, L., Eichler, T., & Rosell, J. (1998). *Differential Mobility Analysis of Molecular Ions and nanometer Particles.* TrAC Trends in Analytical Chemistry, 17, 328–339.

Department of Health and Human Services (DHHS). (2003). *Guidance for Filtration Air Cleaning System to Protect Building Environments from Airborne Chemical, Biological, and Radiological Attacks.* Publication 2003–136.

Donaldson, K., Stone, V., Clouter, A., Renwick, L., & MacNee, W. (2001). *Ultrafine Particles.* Journal of Occupational and Environmental Medicine, 58, 211–216.

Dockery, D.W., & Pope, A.C. (1994). *Acute Respiratory Effects of Particulate Air Pollution.* Annual Review of Public Health. 15, 107–132.

Dullien, F.A.L. (1989*). Introduction to Industrial Gas Cleaning,* Academic Press, San Diego.

Eninger, R.M., Honda, T., Adhikari, A., Tanski, H., Reponen, T., & Grinshpun, S.A. (2008). *Filter Performance of N99 and N95 Face-Piece Respirators against Viruses and Ultrafine Particles.* Annals of Occupational Hygiene, 52, 385–396.

Ensor, D.S., & Hanley, J.T. (1997). Recent Advances in Particulate Air Filter Testing: Quality Assurance Framework; issue of Air Media.

Fjeld, R. & Owens, T. (1988). *The Effect of Particle Charge on Penetration in an Electret Filter.* IEEE Transactions on Industry Applications, 24, 725–731.

Hagdnagy, W., Stiller-Winkler, R., Kainka, R., Ranft, U., & Idel, H. (1998). *Influence of Urban Air Pollution on the Immune System of Children.* Journal of Aerosol Science, Supplement 2, S997–S998.

Han, D.H. (2000). *Performance of Respirator Filters Using Quality Factor in Korea.* Industrial Health Journal, 38, 380–384.

Hinds, W.C. (1999). *Aerosol Technology: Properties, Behavior, and Measurement of Airborne Particles.* (2nd ed.), NewYork: Wiley.

Huang, S.H., Chen, C.W., Chang, C.P., Lai, C. Y., & Chen, C.C. (2007). *Penetration of 4.5 nm to 10 µm Aerosol Particles through Fibrous Filters.* Journal of Aerosol Science, 38, 719–727.

Ikezaki, K., Iritani, K., Nakamura, T., & Hori, T. (1995). *Effect of Charging State of Particles on Electrets.* Journal of Electrostatics, 35, 41–46.

Ichitsubo, H., Hashimoto, T., Alonso, M., & Kousaka, Y. (1996). *Penetration of Ultrafine Particles and Ion Clusters through Wire Screens.* Journal of Aerosol Science, 24, 119–127.

Janssen, L. (2003). *Principles of Physiology and Respirator Performance.* Occupational Health & Safety, 72, 73–81.

Japuntich, D.A., Franklin L., Pui, D.Y.H., Kuehn, T., Kim, S.C., & Viner, A.S. (2007). *A Comparison of Two Nano-Sized Particle Air Filtration Tests in the Diameter Range of 10 to 400 nm.* Journal of Nanoparticle Research, 9, 93–107.

Ji, J.H., Bae, G.N., Kang, S.H., & Hwang, J. (2003). *Effect of Particle Loading on the Collection Performance of an Electret Cabin Air Filter for Submicron Aerosols.* Journal of Aerosol Science, 34, 1493–1504.

Kim, C.S., Bao, L., Okuyama, K., Shimada, M., & Niinuma, H. (2006). *Filtration Efficiency of a Fibrous Filter for Nano-Particles.* Journal of Nanoparticle Research, 8, 215–221.

Kim, S., Harrington, M., & Pui, D. (2007). *Experimental Study of Nano-Particles Penetration through Commercial Filter Media*. Journal of Nanoparticle Research, 9, 117–125.

Kousaka, Y., Okuyama, K., Shimada, M., & Takii, Y. (1990). *Development of a Method for Testing Very High-Efficiency Membrane Filters for Ultrafine Aerosol Particles.* Journal of Chemical Engineering of Japan, 23, 568–574.

Lee, K.W., & Liu, B. (1980). *On the Minimum Efficiency and the Most Penetrating Particle Size for Fibrous Filters.* Journal of the Air Pollution Control Association, 30, 377–381.

Lowkis, B., & Motyl, E. (2001). *Electret Properties of Polypropylene Fabrics.* Journal of Electrostatics, 51-52, 232–238.

May, K.R. (1973). *The Collison Nebulizer Description, Performance & Application.* Journal of Aerosol Science, Vol. 4, #3, pp. 235.

McCullough, N.V., Brosseau, L.M., & Vesley, D. (1997). *Collection of Three Bacterial Aerosols by Respirator and Surgical Mask Filters under Varying Conditions of Flow and Relative Humidity.* Annals of Occupational Hygiene, 41, 677–690.

Miguel, A.F. (2003). *Effect of Air Humidity on the Evolution of Permeability and Performance of a Fibrous Filter during Loading with Hygroscopic and Non-Hygroscopic Particles.* Journal of Aerosol Science, 34, 783–799.

Martin, S.B. & Moyer, E.S. (2000). *Electrostatic respirator filter media: filter efficiency and most penetrating particle size effects.* Applied occupational and Environmental Hygiene 15, 609–617.

Moyer, E.S., & Stevens, G.A. (1989). *''Worst Case'' Aerosol Testing Parameters: II. Efficiency Dependence of Commercial Respirator Filters on Humidity Pretreatment.* American Industrial Hygiene Association Journal, 50, 265–270.

National Institute for Occupational Safety and Health (NIOSH) and the Bureau of Labor Statistics (BLS). (2003), *Respirator Usage in Private Sector Firms.* Department of Health and Human Services& Department of Labor.

Nemmar, A., Vanbilloen, H., Hoylaerts, M., Hoet, P., Verbruggen, A., & Nemery, B. (2001). *Passage of Intratracheally Instilled Ultrafine Particles from the Lung into the Systemic Circulation in Hamster.* American Journal of Respiratory and Critical Care Medicine, 164, 1665–1668.

Nemmar, A., Hoet, P., Vanquickenborne, B., Dinsdale, D., Thomeer, M., Hoylaerts, MF., Vanbilloen, H., Mortelmans, L., & Nemery, B. (2002). *Passage of Inhaled Particles into the Blood Circulation in Humans.* Circulation, 105, 411–414.

Oberdorster, G. (2000). *Toxicology of Ultrafine Particles: in Vivo Studies.* Philosophical Transactions of the Royal Society A, 358, 2719–2740.

Oberdorster, G., Sharp, Z., Atudorei, V., Elder, A., Gelein, R., Lunts, A., Kreyling, W., & Cox, C. (2002). *Extrapulmonary Translocation of Ultrafine Carbon Particles Following Whole-Body Inhalation Exposure of Rats.* Journal of Toxicology and Environmental Health, Part A, 65, 1531–1543.

Oberdorster, G., Sharp, Z., Atudorei, V., Elder, A., Gelein, R., Kreyling, W., & Cox, C. (2004). *Translocation of Inhaled Ultrafine Particles to the Brain.* Inhalation Toxicology, 16, 437–445.

Oberdorster, G. (2005). *Nanotoxicology: An Emerging Discipline Evolving from Studies of Ultrafine Particles.* Environmental Health Perspectives, 113, 823–839.

Ostiguy, C., Soucy, B., Lapointe, G., Woods, C. et Ménard, L. (2008). Les Effets Sur La Santé Reliés Aux Nano-Particules, Rapport IRSST R–558, 2e édition.

Otani, Y., Cho, S.J. & Emi, H. (1994). *Removal of Nanometer Size Particles and Ions from Air.* Proceedings of the 12th ISCC, Yokohama, Japan, pp. 21–25.

Pui, D.Y.H. & Kim, S.C. (2006). *Penetration of Nano-Particles through Respirator Filter Media.* Final Report NIOSH Contract No. 254–2005–M–11698, Mechanical Engineering Department University of Minnesota.

Rengasamy, S., Verbofsky, R., King, W.P., Eimer, B.C., & Shaffer, R.E. (2007). *Nano-Particle Penetration through NIOSH-Approved N95 Filtering Face-Piece Respirators.* Journal of the International Society for Respiratory Protection, 24, 49–59.

Rengasamy, S., King, W.P., Eimer, B.C., & Shaffer, R.E. (2008a). *Filtration Performance of NIOSH-Approved N95 and P100 Filtering Face-Piece Respirators against 4 to 30 Nanometer-Size Nano-Particles.* Journal of Occupational and Environmental Hygiene, 5, 556–564.

Rengasamy, S., Eimer, B.C., & Shaffer, R.E. (2008b). *Nano-Particle Filtration Performance of Commercially Available Dust Masks.* Journal of the International Society for Respiratory Protection, 25, 27–41.

Richardson, A.W., Eshbaugh, J.P. Hofacre, K.C. & Gardner, P.D. (2006). *Respirator Filter Efficiency against Particulate and Biological Aerosols under Moderate to High Flow Rates.* U.S. Army Edgewood Chemical Biological Center Report for Contract No. SP0700-00-D-3180.http://www.cdc.gov/niosh/npptl/researchprojects/pdfs/CR–085Gardner.pdf.

SCENIHR. (2006). *The Appropriateness of Existing Methodologies to Assess the Potential Risks Associated with Engineered and Adventitious Products of Nanotechnologies.* Directorate C–Public Health and Risk Assessment. C7–Risk Assessment. Scientific Committee on Emerging and Newly Identified Health Risk.

Shin, W.G., Mulhollandb, G.W., Kim, S.C., & Pui, D.Y.H. (2008). *Experimental Study of Filtration Efficiency of Nano-Particles below 20 nm at Elevated Temperatures.* Jounral of Aerosol Science, 39, 488–499.

Steffens, J. & Coury, J.R. (2007). *Collection Efficiency of Fiber Filters Operating on the Removal of Nano-Sized Aerosol Particles: I–Homogeneous Fibers.* Separation and Purification Technology 58, 99–105.

Takenaka, S., Karg, D., Roth, C., Schulz, H., Ziesenis, A., Heinzmann, U., Chramel, P., & Heyder, J. (2001). *Pulmonary and Systemic Distribution of Inhaled Ultrafine Silver Particles in Rats.* Environmental Health Perspectives, 109, 547–551.

The National Air Filtration Association (NAFA). (2007). *Method of Testing General Ventilation Air-Cleaning Devices for Removal Efficiency by Particle Size.* User's Guide for ANSI/ASHRAE 52.2. http://www.nafahq.org/LibaryFiles/Articles/Article006.htm. Accessed July 20, 2008.

Tran, CL., Buchanan, D., & Cullen, RT. (2000*). Inhalation of Poorly Soluble Particles. II. Influence of Particle Surface Area on Inflammation and Clearance.* Inhalation Toxicology, 12, 1113–1126.

TSI. (2003). *Model 3012A Aerosol Neutralizer Instructions.* TSI Incorporated.

TSI. (2005). *Model 3936 Scanning Mobility Particle Sizer Spectrometer Instructions.* TSI Incorporated.

Wang, H., & Kasper, G. (1991). *Filtration Efficiency of Nanometer-Size Aerosol Particles.* Journal of Aerosol Science, 22, 31–41.

Wang, C.S. (2001). *Electrostatic Forces in Fibrous Filters- A Review.* Powder Technology, 118, 166–170.

Warheit, D.B., Webb, T.R., Colvin, V.L., Reed, K.L., & Sayes, C. M. (2007a). *Pulmonary Bioassay Studies with Nanoscale and Fine-Quartz Particles in Rats: Toxicity Is Not Dependent Upon Particle Size But on Surface Characteristics.* Toxicological Sciences, 95, 270–280.

Warheit, D.B., Webb, T.R., Reed, K.L., Frerichs, S., & Sayes, C. M. (2007b). *Pulmonary Toxicity Study in Rats with Three Forms of Ultrafine-TiO2 Particles: Differential Responses Related to Surface Properties.* Toxicological Sciences, 230, 90–104.

Wiedensohler, A. (1998). *An Approximation of the Bipolar Charge Distribution for Particles in the Submicron Size Range.* Journal of Aerosol Science, 19, 387–389.

Woon, W., Leung, F., & Hunga, C.H. (2008*). Investigation on Pressure Drop Evolution of Fibrous Fiter Operating in Aerodynamic Slip Regime under Continuous Loading of Sub-Micron Aerosols.* Separation and Purification Technology, 63, 691–700.

Yang, S., & Lee, G.W.M. (2005). *Filtration Characteristics of a Fibrous Filter Pretreated with Anionic Surfactants for Mono-disperse Solid Aerosols.* Journal of Aerosol Science, 36, 419–437.

APPENDIX A: AEROSOL GENERATION SYETEM

The aerosol generation systems should have a good particle size distribution and a stable particle output. Three major measurement techniques are commonly applied in aerosol research studies as a generation system. These techniques are: Electro-Spray, Jet Collision Nebulizer and Traditional Evaporation Condensation Method.

In this study, due to its simplicity and efficiency, the Jet Collision Nebulizer technique has been employed for generating submicron aerosols, fed with sodium chloride, to challenge N95 filtering face-piece respirators. This generation system technique has been first used by Collision in 1935 in the scientific investigations (May, 1973). As shown in figure A-1, after passing a compressed- clean air through the liquid (supplied in 1 liter glass jar), the solution is drawn into high velocity jet section, where it is atomized and evaporated in to droplets. Then, to remove the large droplets coming out from the jet section, the liquid/gas is impacted with a barrier across from the jet. Finally, the sprayed droplets exit the atomizer from the aerosol outlet at top. For more detailed information, see the BGI manual for the 3, 6 and 24- Jets Collision Nebulizer.

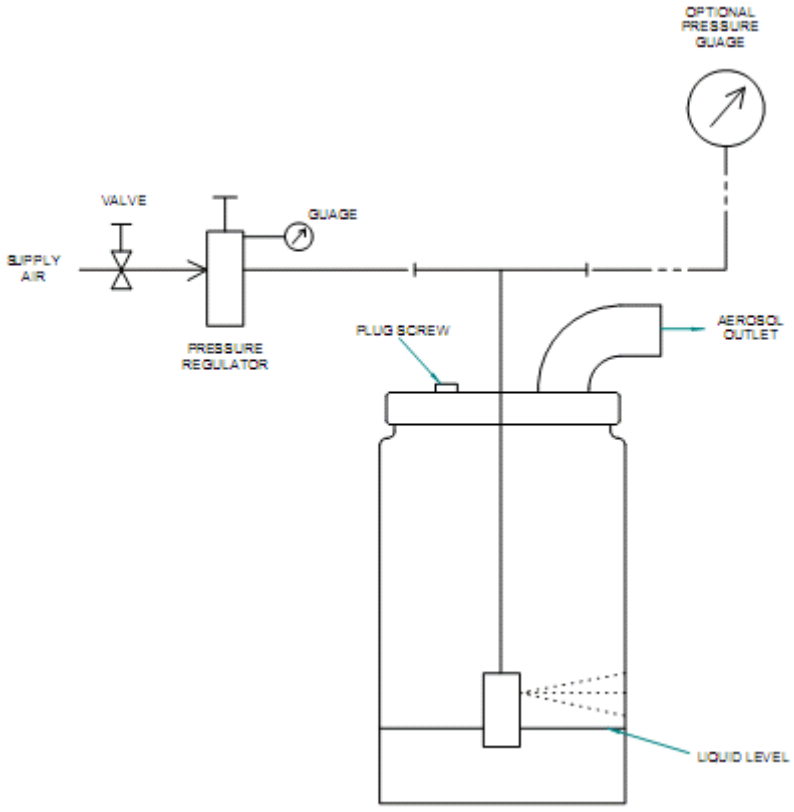

Figure A-1: Schematic digram of Collision Nebilizer model Waltham. MA. Adapted from BGI, Inc., 2002.

APPENDIX B: NANO-PARTICLE MEASURING INSTRUMENT

Various measurement techniques have been developed to determine the characteristics of NPs. These methods include: mass concentration, number concentration and size distribution. As mentioned earlier, the Scanning Mobility Particle Sizer (SMPS) has been employed in this study to measure the particle concentration and size distribution based on the particle electrical mobility (inversely proportion to the particle diameter). This advanced technique is capable to measure particles ranged from 4 to 10000 nm.

The SMPS mainly consists of particle size classifier (Electrostatic classifier with DMA) and particle detector (UCPC). Particle size classifier classifies the charged particles based on their electrical mobility (or electrical mobility diameter). Particles with a narrow range of electrical mobility are able to exit from DMA and then counted by the Ultrafine Condensation Particle Counter (UCPC).

Particle Size Classifier

Figure B-1 shows the schematic diagram of the electrostatic classifier with long DMA (model 3081, TSI Inc.). In this system, to provide a bipolar equilibrium charge on the aerosols, the aerosol flow is first passed through a radioactive bipolar charger in the Electrostatic Classifier before entering the DMA. Then, the particles are selected in DMA according to their electrical mobility.

As shown in the figure, the DMA contains an outer, grounded cylinder and an inner cylindrical electrode which is connected to a negative power supply (0 to 10 KV- DC). The electric field between the two concentric cylinders separates the particles according to their electrical mobility (which is inversely related to the particle size). Particles with the negative charge(s) are deposited on the outer wall, whereas those with positive charge(s) move rapidly towards the negatively- charged center electrode. Only size selected particles within a narrow range of electrical mobility have the correct trajectory to exit DMA. The electrical mobility of these selected particles is affected by various parameters including the flow rates, geometric parameters and the voltage of the center electrode. The size selected particle stream exiting from DMA is then counted by the Ultrafine Condensation Particle Counter (UCPC).

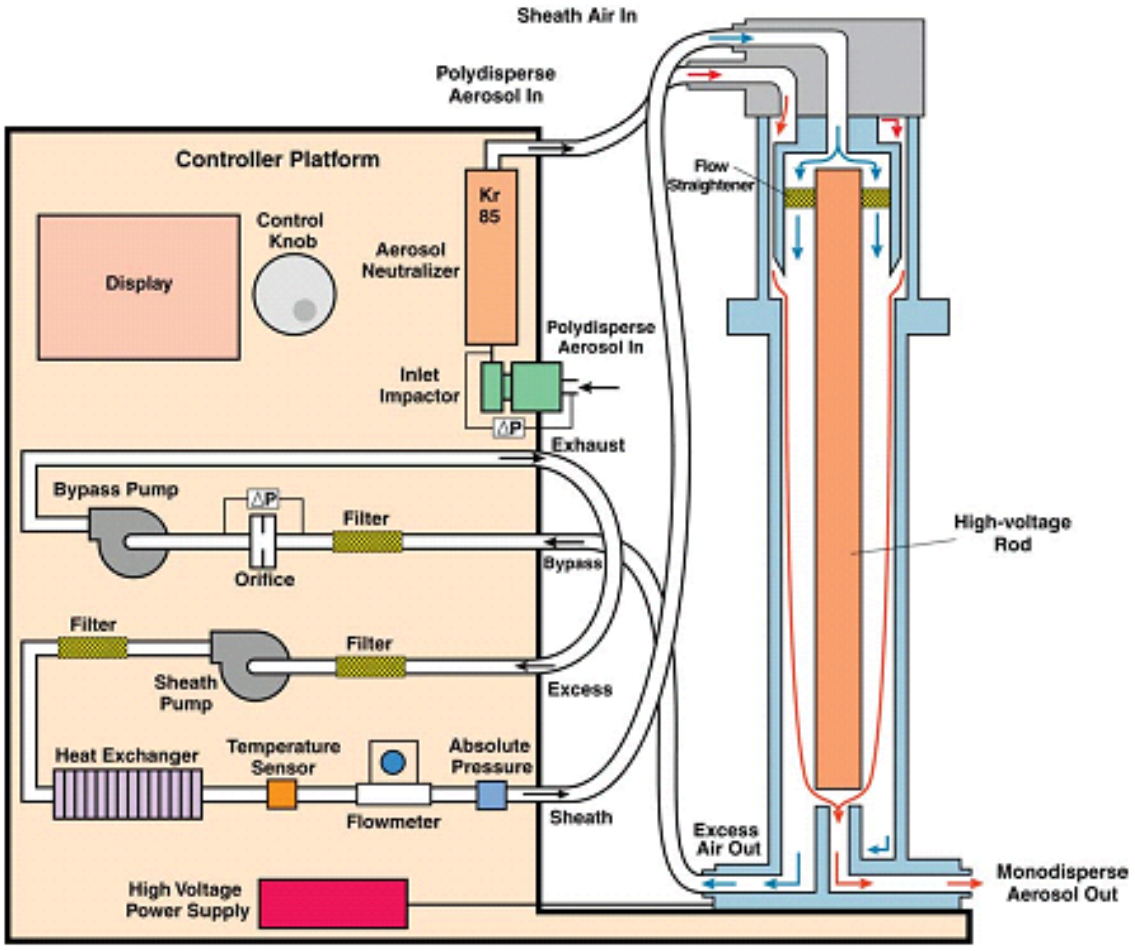

Figure B-1: Schematic diagram of the Electrostatic classifier with long DMA, model 3081. Adapted from TSI Inc., 2005.

Particle size distributions are measured by changing the voltage between the inner and outer cylindrical electrodes in the DMA, which changes the electrical field. DMA voltage (V) is corresponded to the electrical mobility, Z, and mobility diameter, d, by the following equation:

$$Z = \frac{Q \ln(\frac{R_2}{R_1})}{2\Pi LV} = \frac{0.441 \left(\frac{k_B T}{M}\right)^{0.5}}{pd^2}$$

Where R_1 and R_2 are the inner and outer radius of the DMA, L is the DMA length from inlet to outlet slit, Q is the carrier gas flow rate, k is the Boltzmann constant, and T, p, and M are the temperature, pressure and molecular weight of the carrier gas (Fernandez de la Mora et al., 1998). For more specific information, review the TSI manual for series 3080 electrostatic classifiers.

Ultrafine Condensation Particle Counter (UCPC)

Ultrafine Condensation particle counter (UCPC) is normally used as a part of Scanning Mobility Particle Sizer (SMPS) to count the number of particles greater than a few nanometers in diameter. Particle detection and counting is provided by a simple optical detector after a supersaturated vapor of 1-butanol condenses on the particles, causing them to grow larger.

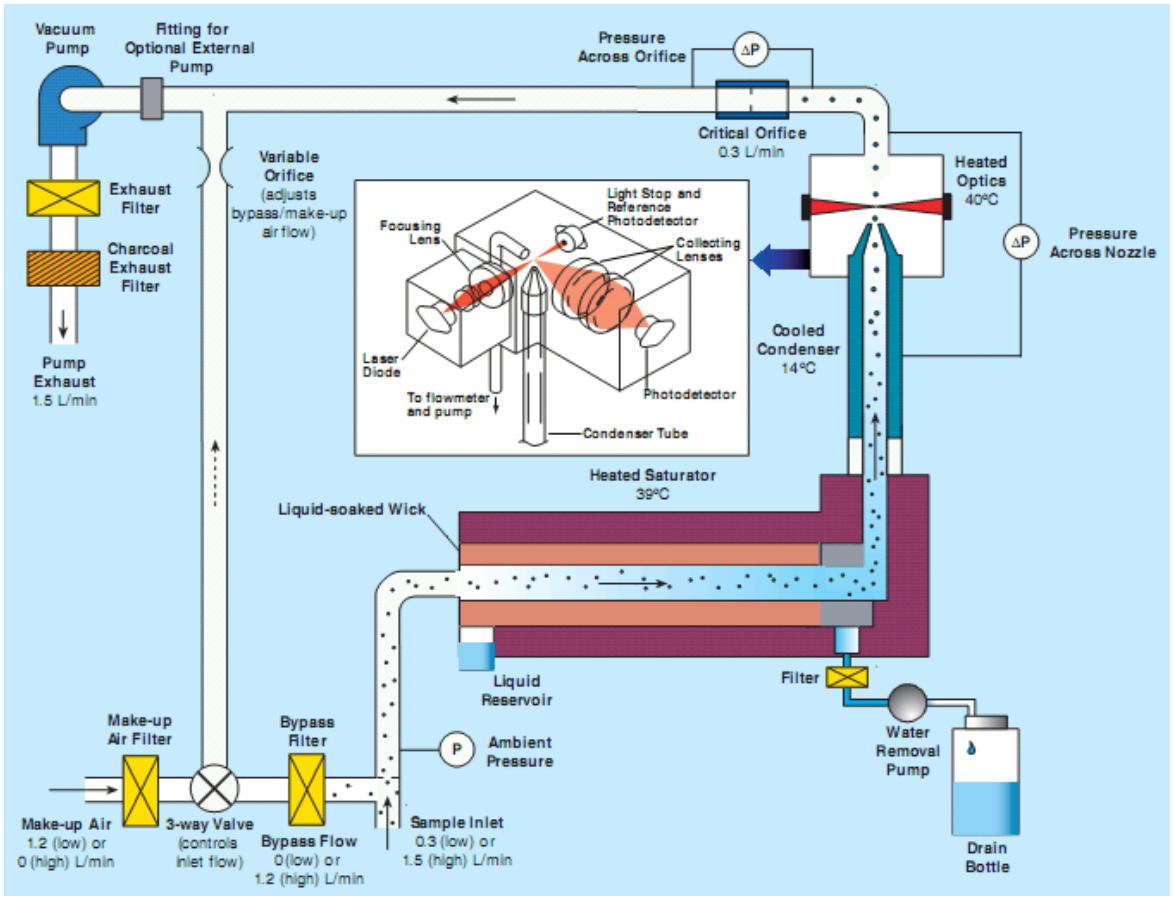

Figure B-2: Schematic diagram of Ultrafine Condensation Particle Counter, model 3775. Adapted from TSI Inc., 2005.

In the UCPC, single particles larger than 2 nm are grown to micrometer size by means of condensation of a fluid (alcohol or water) on the particles. The CPC then optically counts these particles. For more detailed information, review the TSI manual for the Ultrafine Condensation Particle Counter (UCPC), model 3775.

APPENDIX C: PARTICLE NEUTRALIZER

To evaluate the filtration efficiency tests in a worst case scenario, the particles are required to be charge neutralized before entering the test chamber. This is especially vital when the generated particles carry a considerable amount of charge. To minimize this problem, a neutralizer instrument (3012A Model, TSI Inc.) is applied to either eliminate or reduce the possible positive and negative charges carried by the particles.

As the particles enter the neutralizer, they become exposed to the positive and negative air ions. The air ions are attracted to the oppositely charged particles causing the level of possible charge on the particles to reduce significantly.

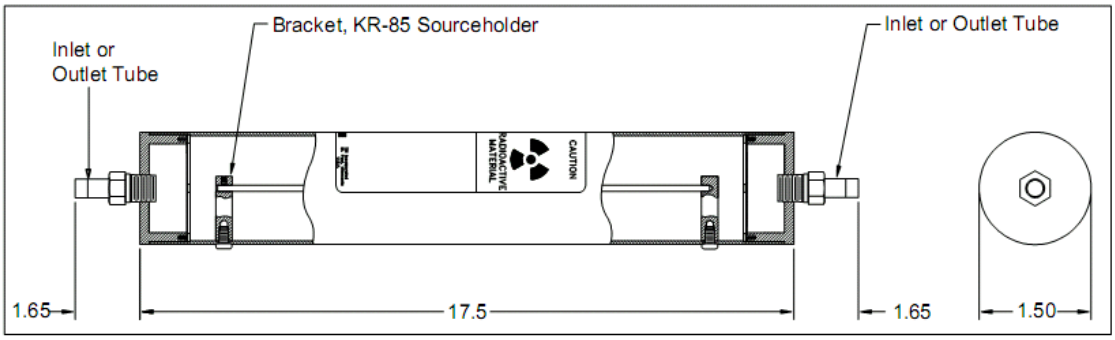

Figure C-1: Model 3012A Aerosol Neutralizer. Adapted from TSI Inc., 2003.

By providing sufficient residence time, the Boltzmann charge equilibrium will be obtained for the particles. The following table displays an approximation of the charge distribution for the particles in nano size range, carried out by the Wiedensohler, (1998). In spite of particle neutralization, a portion of the particles still carry some charges which becomes greater at larger particle size. Notes, the 3012A model aerosol neutralizer

applies a radioactive source (10 milligrams of Kr-85) to provide negative and positive air ions.

Table C-1: Distribution of charges on aerosol according to Gunn Formula (Wiedensohler,1998).

	Percent of Particle Carrying Np Elementary Charge Units												
Dp(μm)	-6	-5	-4	-3	-2	-1	0	+1	+2	+3	+4	+5	+6
0.01						5.14	90.75	4.11					
0.02					0.02	10.96	80.57	8.64	0.01				
0.04					0.54	19.50	64.79	14.86	0.31				
0.06				0.02	1.92	24.32	54.13	18.51	1.09	0.01			
0.08				0.11	3.72	26.81	46.73	20.46	2.10	0.05			
0.10				0.37	5.63	27.31	42.28	20.91	3.30	0.17			
0.20		0.05	0.53	3.40	12.38	25.49	29.66	19.51	7.26	1.53	0.18	0.01	
0.40	0.27	1.14	3.60	8.54	15.24	20.46	20.65	15.66	8.93	3.83	1.24	0.03	0.05
0.60	1.21	3.00	6.19	10.53	14.82	17.25	16.60	13.20	8.69	4.73	2.13	0.79	0.24
0.80	2.42	4.64	7.71	11.12	13.90	15.06	14.15	11.53	8.15	4.99	2.65	1.22	0.49
1.00	3.56	5.84	8.53	11.13	12.96	13.45	12.46	10.30	7.59	5.00	2.93	1.54	0.92

APPENDIX D: PARTICLE SIZE DISTRIBUTION AT UPSTREAM

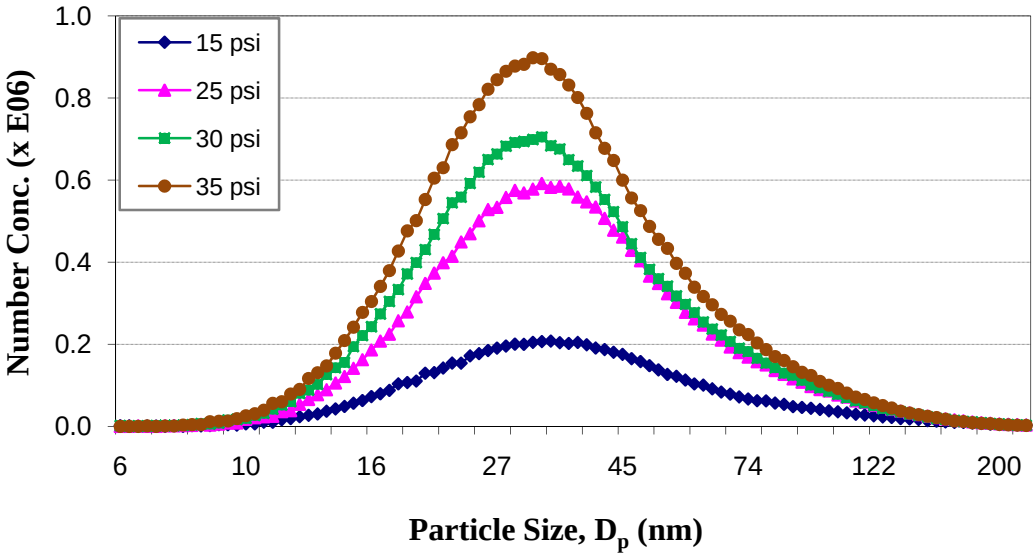

Figure D-1: Particle concentration as a function of particle size at different pressures (135 liters/min and 0.01% NaCl solution).

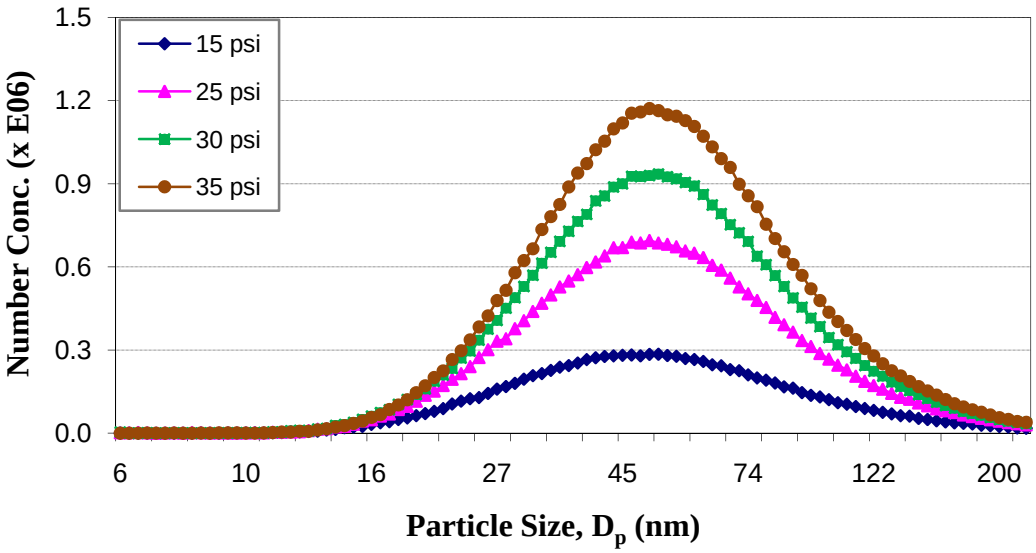

Figure D-2: Particle concentration as a function of particle size at different pressures (135 liters/min and 0.1% NaCl solution).

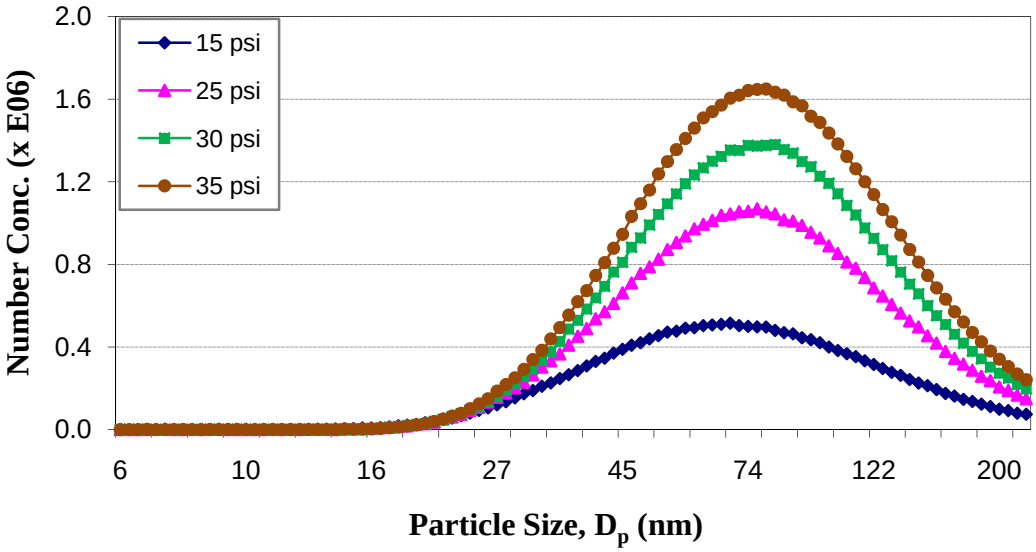

Figure D-3: Particle concentration as a function of particle size at different pressures (135 liters/min and 0.1% NaCl solution).

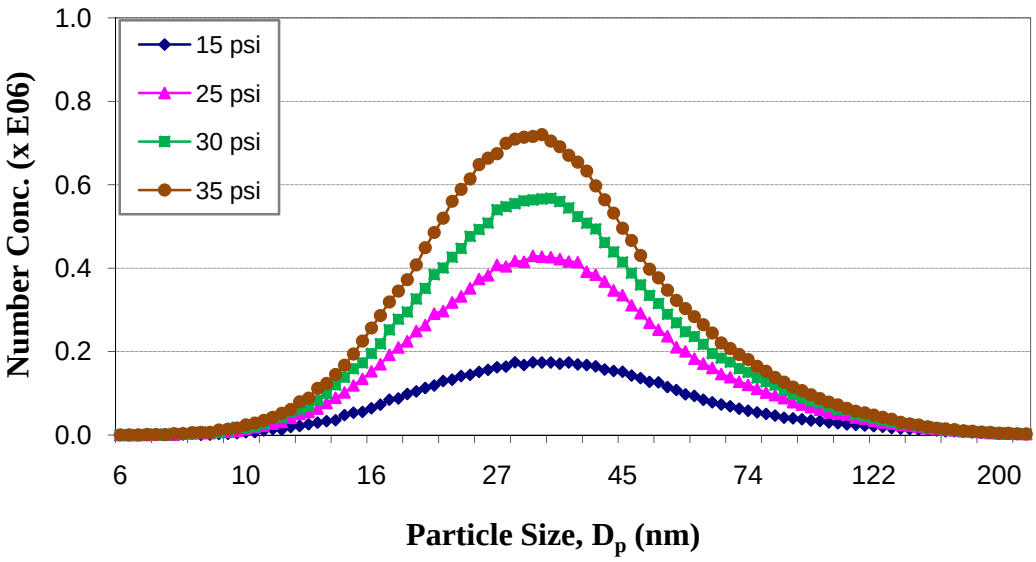

Figure D-4: Particle concentration as a function of particle size at different pressures (270 liters/min and 0.01% NaCl solution).

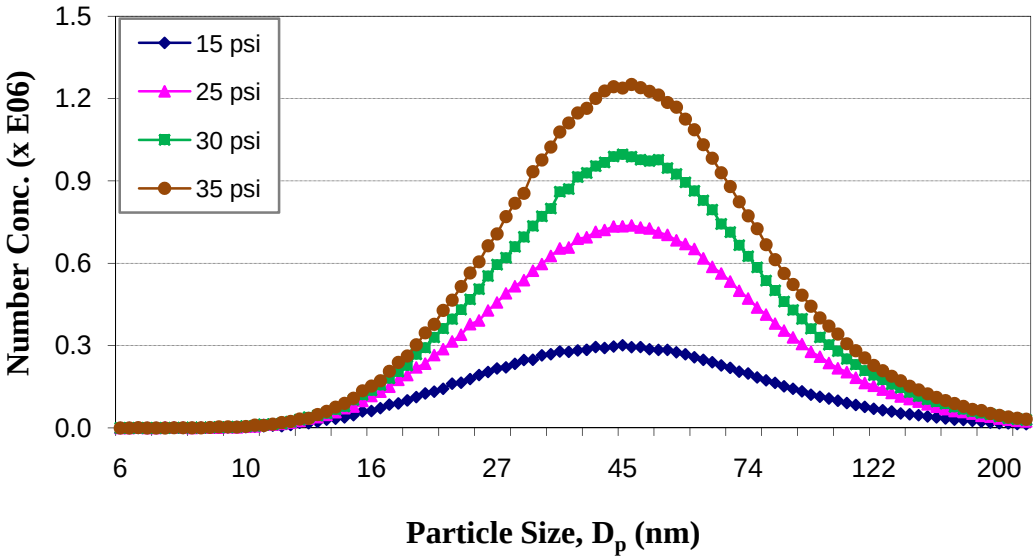

Figure D-5: Particle concentration as a function of particle size at different pressures (270 liters/min and 0.1% NaCl solution).

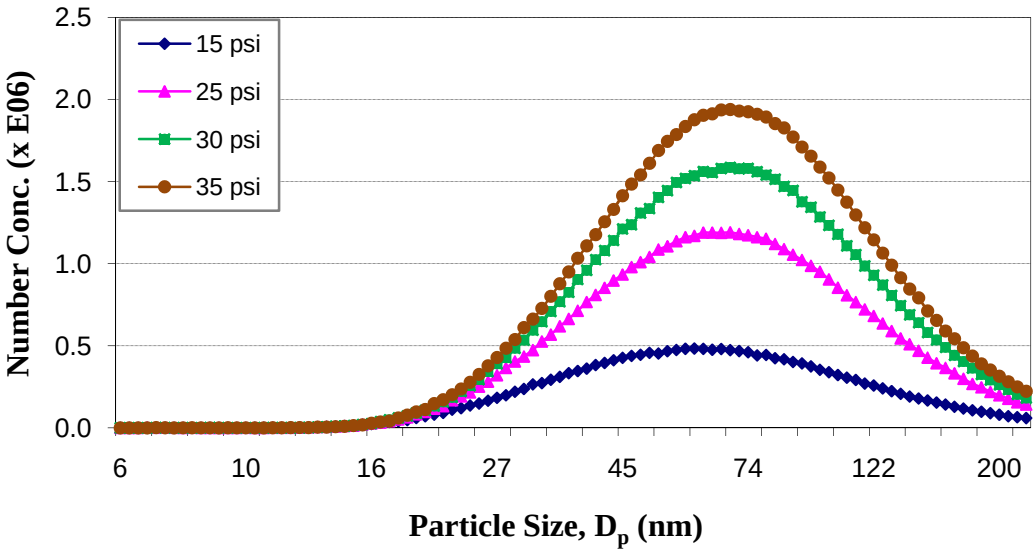

Figure D-6: Particle concentration as a function of particle size at different pressures (270 liters/min and 1% NaCl solution).

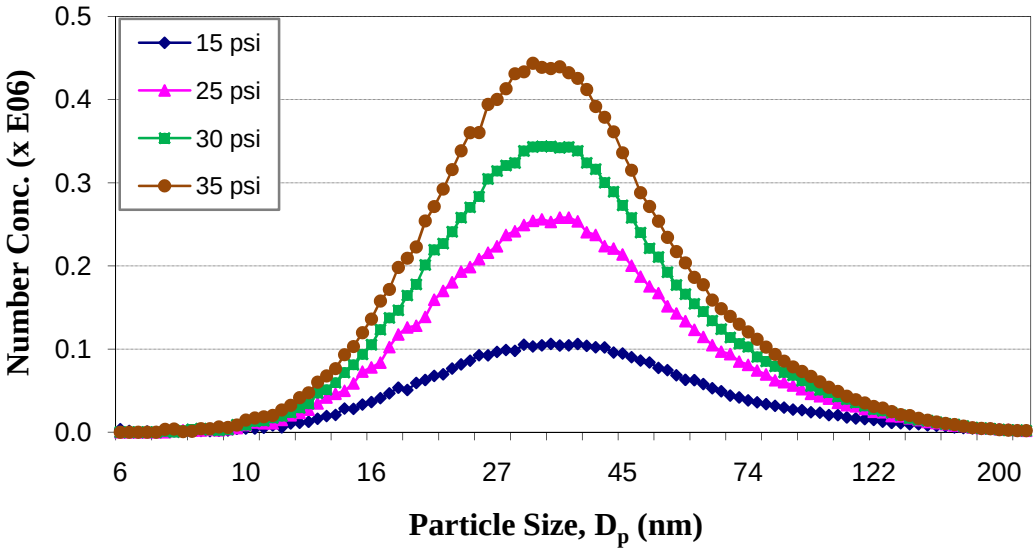

Figure D-7: Particle concentration as a function of particle size at different pressures (360 liters/min and 0.01% NaCl solution).

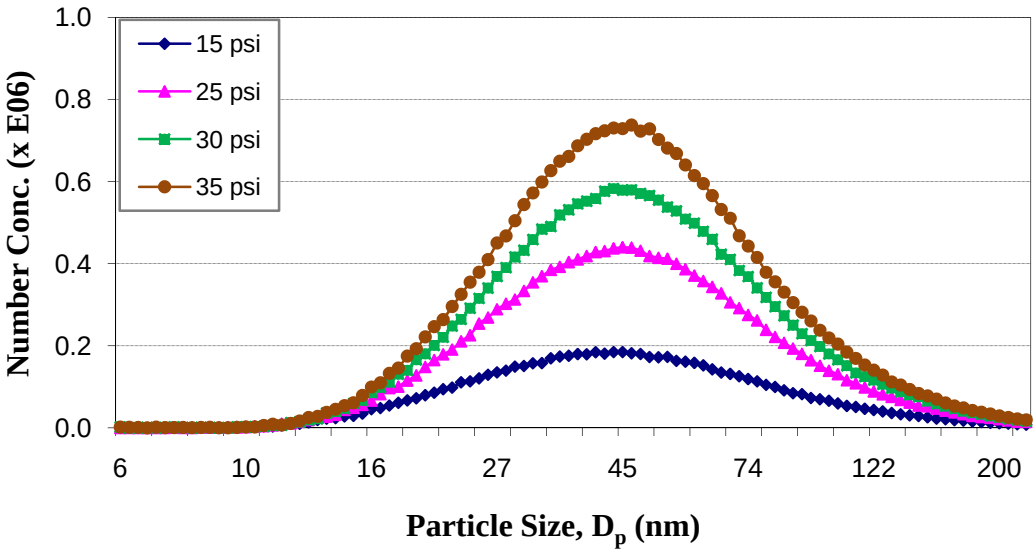

Figure D-8: Particle concentration as a function of particle size at different pressures (360 liters/min and 0.1% NaCl solution).

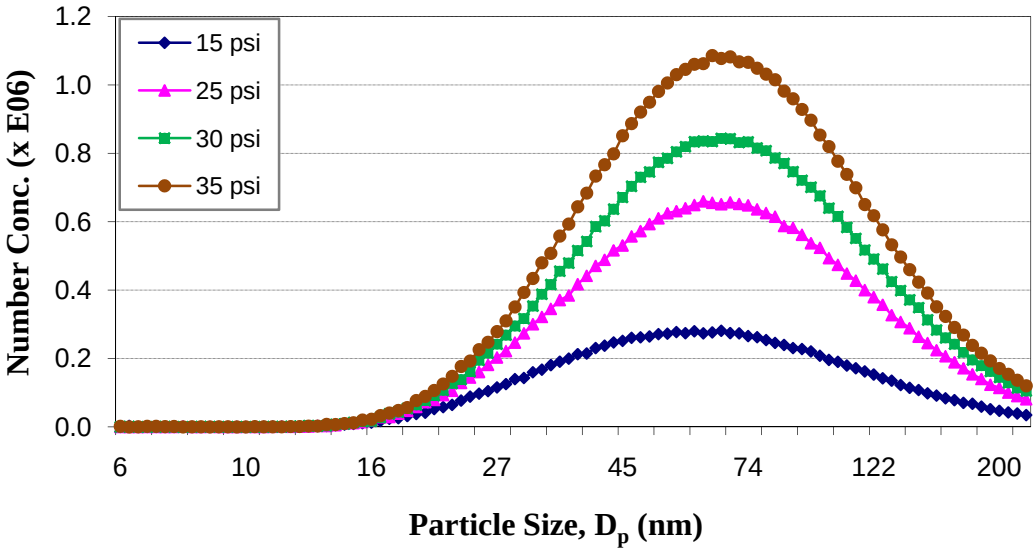

Figure D-9: Particle concentration as a function of particle size at different pressures (360 liters/min and 1% NaCl solution).